
When Heterophily Meets Heterogeneity: New Graph Benchmarks and Effective Methods

Junhong Lin¹ Xiaojie Guo² Shuaicheng Zhang³

Dawei Zhou³ Yada Zhu² Julian Shun¹

¹MIT CSAIL ²IBM Research ³Virginia Tech

junhong@mit.edu, Xiaojie.Guo@ibm.com, zshuai8@vt.edu

zhoud@vt.edu, yzhu@us.ibm.com, jshun@mit.edu

Abstract

Many real-world graphs frequently present challenges for graph learning due to the presence of both heterophily and heterogeneity. However, existing benchmarks for graph learning often focus on heterogeneous graphs with homophily or homogeneous graphs with heterophily, leaving a gap in understanding how methods perform on graphs that are both heterogeneous and heterophilic. To bridge this gap, we introduce $\mathcal{H}^2\text{GB}$, a novel graph benchmark that brings together the complexities of both the heterophily and heterogeneity properties of graphs. Our benchmark encompasses 9 diverse real-world datasets across 5 domains, 28 baseline model implementations, and 26 benchmark results. In addition, we present a modular graph transformer framework UNIFIEDGT and a new model variant, $\mathcal{H}^2\text{G-former}$, that excels at this challenging benchmark. By integrating masked label embeddings, cross-type heterogeneous attention, and type-specific FFNs, $\mathcal{H}^2\text{G-former}$ effectively tackles graph heterophily and heterogeneity. Extensive experiments across 26 baselines on $\mathcal{H}^2\text{GB}$ reveal inadequacies of current models on heterogeneous heterophilic graph learning, and demonstrate the superiority of our $\mathcal{H}^2\text{G-former}$ over existing solutions. Both the benchmark and the framework are available on Github and PyPI, and documentation can be found at <https://junhongmit.github.io/H2GB/>.

1 Introduction

Graphs are increasingly prevalent in the real world due to their ability to model complex relationships across various domains, such as finance [65], social science [61, 35] and cybersecurity [23, 67]. Graph neural networks (GNNs) [22, 32] have been pivotal in achieving state-of-the-art performance on a wide range of graph learning tasks. GNNs were primarily designed for homogeneous graphs, which have a single type of node and edge, and used a neighborhood aggregation scheme to capture structural information [17]. Furthermore, the neighbor aggregation function used in many existing GNNs typically assumes that the graph is homophilic, i.e., connected nodes are similar to each other [83]. We say that these methods focus on *homogeneous homophilic graphs*, as shown in Figure 1(a).

However, many real-world graphs, such as academic networks [78, 28], social networks [61], and financial networks [55, 4], frequently present challenges for graph learning due to *heterophily*, where connected nodes may have dissimilar labels and attributes, and *heterogeneity*, where multiple types of entities and relations among the graphs are embodied by various types of nodes and edges. Each of these two properties can significantly impede the performance of GNNs. In recent years, researchers have actively explored methods to overcome these challenges in two separate directions. (1) To handle graphs with heterophily, there has been a recent line of research on developing heterophilic graph benchmarks [7, 41] and heterophily-centered GNNs [83, 44, 52, 84, 7] that incorporate long-range relationships and distinct aggregation mechanisms, such as distant node exploration [83, 52, 1, 40], signed aggregation [7, 84, 44], and local grouping [40]. However, these heterophilic GNNs are

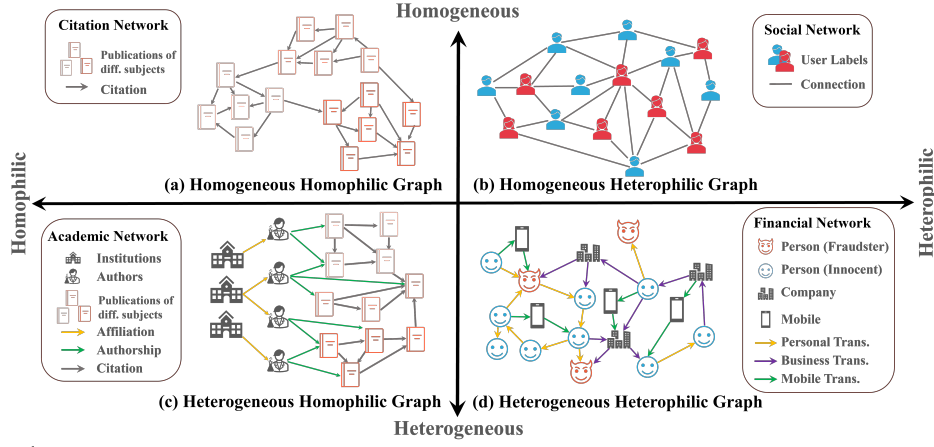


Figure 1: Examples of graphs with different levels of heterophily and heterogeneity. The nodes with different class labels and edges of different types are represented with different colors (e.g., publications of different subjects or different kinds of financial transactions).

restricted to homogeneous graphs, as illustrated in Figure 1(b). (2) Heterogeneous GNNs have been proposed to handle the diverse information hidden in heterogeneous graphs [57, 77, 66, 15, 25, 29]. However, most heterogeneous GNNs are built upon the homophily assumption, as illustrated in Figure 1(c), and exhibit poor performance on heterophilic graphs.

While there have been advancements in handling heterophily and heterogeneity separately, there is a lack of research on learning on graphs with both of these properties, which many real-world graphs exhibit. For example, financial networks (Figure 1(d)) [55, 4] are both heterophilic and heterogeneous. Different node types (person, business, etc.) and edge types (wire transfer, credit card transaction, etc.) exist, making the graph heterogeneous. Furthermore, the class labels of fraudsters differ from those of their innocent neighbors, making the graph heterophilic. Graphs from other domains can also be both heterophilic and heterogeneous, including graphs from e-commerce [42], academia [78, 28], and cybersecurity [34, 5]. Thus, it is important to develop graph learning methods for this setting where both heterophily and heterogeneity exist.

The following challenges arise when exploring graph learning in heterophilic and heterogeneous settings. (1) **Lack of Benchmarks on Graphs with both Heterophily and Heterogeneity:** Existing benchmarks either focus exclusively on homogeneous graphs, neglecting the diversity of node and edge types found in real-world graphs, or on heterogeneous graphs while assuming homophily. (2) **Ineffective Heterophily Measures in Heterogeneous Contexts:** The standard graph heterophily metrics are defined for homogeneous graphs, and fall short for heterogeneous graphs, particularly in the presence of class imbalance. This inadequacy prevents a thorough understanding and effective handling of heterogeneous heterophilic graphs. (3) **Inadequacy of Heterophilic GNNs for Heterogeneous Graphs:** GNNs that are optimized for heterophilic graphs typically neglect heterogeneous information, leading to underperformance when both heterophily and heterogeneity are present.

To address these gaps, we introduce a novel graph benchmark, the **Heterophilic and Heterogeneous Graph Benchmark ($\mathcal{H}^2\text{GB}$)**, which is designed to evaluate graph learning methods in both heterophilic and heterogeneous settings. As shown in Figure 2, $\mathcal{H}^2\text{GB}$ includes 9 real-world datasets across 5 diverse domains: academia, finance, e-commerce, social science, and cybersecurity. $\mathcal{H}^2\text{GB}$ covers multiple real-world applications: paper venue classification, financial fraud/malware detection, and social network analysis. Additionally, most of the datasets are large, containing millions of nodes and tens of millions of edges (see Table 1), which are orders of magnitude larger than existing heterophilic benchmarks [81, 41]. Thus, $\mathcal{H}^2\text{GB}$ is useful in evaluating the scalability of graph learning methods.

In addition, to summarize and systematically compare the performance of existing GNNs on this new benchmark, we propose UNIFIEDGT, a modular graph transformer (GT) framework. UNIFIEDGT is designed to encompass many existing GTs and GNNs by leveraging modular ingredients (Figure 2): (1) graph sampling, (2) graph encoding, (3) graph attention, (4) attention masking, and (5) feedforward networks (FFN). In this paper, we implement 9 existing GT baselines and 19 GNN models using UNIFIEDGT. Furthermore, to handle graphs with both heterophily and heterogeneity, we introduce a new GT variant, $\mathcal{H}^2\text{G-former}$. This variant enhances existing GTs by incorporating a masked label embedding for the modular graph encoding, a cross-type heterogeneous attention module for

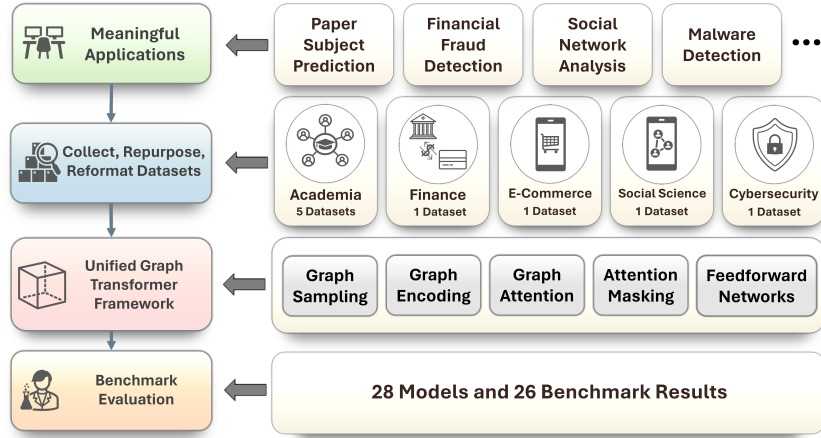


Figure 2: $\mathcal{H}^2\text{GB}$ consists of datasets across various domains (Section 2), a modular UNIFIEDGT framework (Section 3) and 26 benchmark results, making it easy to evaluate methods, and compare performance (Section 4).

modular graph attention, and a type-specific FFN for the modular FFN component. UNIFIEDGT is implemented as a Python library and is user-friendly. It includes a unified data loader and evaluator, making it easy to access datasets, evaluate methods, and compare performance.

Overall, our contributions are as follows:

- **New Problem and Benchmark Collection.** We develop $\mathcal{H}^2\text{GB}$, the first graph benchmark that combines heterophily and heterogeneity across various domains, providing a challenging and realistic evaluation framework for the new problem: *graph learning in the heterophilic and heterogeneous setting*. Standard heterophily metrics defined for homogeneous graphs fall short on heterogeneous graphs, and so we propose a new heterogeneous heterophily measure, the \mathcal{H}^2 index.
- **Modular Framework and Effective Method.** We implement a modular framework UNIFIEDGT that is capable of expressing many existing GTs and can easily modify their components. We present a new variant, $\mathcal{H}^2\text{G-former}$, to effectively handle heterophilic and heterogeneous graphs.
- **Open-source, Reproducible, and Extensible Library.** We provide the framework as an easy-to-use library, enabling users to access the datasets and reproduce all of our experiments. Furthermore, users can easily build their models by using the existing modules or adding new modules.
- **Comprehensive Benchmark Evaluation.** We present a comprehensive evaluation on 26 baselines, underscoring the challenges posed by heterophilic and heterogeneous graphs and highlighting the potential of $\mathcal{H}^2\text{G-former}$ to enhance graph learning applications across diverse domains.

2 Heterophilic and Heterogeneous Graph Benchmark ($\mathcal{H}^2\text{GB}$)

In this section, we present the $\mathcal{H}^2\text{GB}$, a benchmark consisting of 9 datasets (6 new ones and 3 from existing work) spanning 5 diverse industry domains (Figure 2): academia, e-commerce, finance, social science, and cybersecurity. These domains involve meaningful applications, such as paper venue prediction, financial fraud/malware detection, and social network analysis. We also introduce a new heterophily measure that better captures the heterophilic properties of heterogeneous graphs. The benchmark standardizes data loading, data splitting, feature encoding, and performance evaluation, which together enable open and reproducible research on heterophilic and heterogeneous GNNs.¹

2.1 Proposed Datasets

In this subsection, we briefly introduce each domain and its corresponding datasets. Detailed descriptions of the graphs are given in Appendix D.2. Dataset statistics are provided in Table 1.

2.1.1 Academia

Motivation. Academic networks model the dynamics of academic publishing and collaboration, offering a vital lens for studying patterns arising in graphs [27, 28]. Previously, these networks assume that papers connected through citations or co-authorships are likely to belong to similar venues, reflecting a homophilic interaction pattern. However, this assumption overlooks the inherent heterophily that occurs in academic publishing, where papers from the same authors or cited works

¹As a special case, $\mathcal{H}^2\text{GB}$ can also be useful for systematically evaluating existing homogeneous heterophilic GNNs (by simply removing the type information on nodes and edges).

can span diverse venues, introducing heterophily into the network. This combination of heterogeneity and heterophily in academic networks has been underexplored, presenting a gap that we aim to address.

Task. Within this domain, five of our graph datasets focus on different aspects of academic publishing: `ogbn-mag`, `oag-cs`, `oag-eng`, and `oag-chem` are used to predict the published venue of each paper, and `mag-year` is used to predict the year of paper publication.

Dataset Construction. `ogbn-mag` [27] is an existing benchmark for evaluating heterogeneous GNNs. We have adapted it by defining new node labels featuring the publication years and have created the `mag-year` dataset to further study graph heterophily. `oag-cs`, `oag-eng`, and `oag-chem` are also new datasets we developed, extracted from the Open Academic Graph (OAG) [78]. These datasets encompass over 3,000 classes representing various paper venues, and significant highlight graph heterophily as many connected papers are not published in the same venue.

2.1.2 E-commerce.

Motivation. In e-commerce, ensuring the integrity and safety of products is paramount. Many existing datasets, such as the Amazon product co-purchasing network [27, 37] and the Taobao dataset [2], primarily consist of homogeneous entities and relations, and often fail to capture the complex nature of real-world e-commerce interactions. This limitation underscores the need for datasets reflecting the heterophilic and heterogeneous characteristics inherent in e-commerce platforms.

Tasks. The RCDD dataset focuses on risk commodity detection, identifying counterfeit products and prohibited commodities, which is essential in maintaining the integrity of e-commerce platforms.

Dataset Construction. Collected from existing work [42], RCDD is specifically designed to incorporate both heterogeneity and heterophily to address the gap left by existing e-commerce datasets which are homogeneous. This dataset was derived from a large-scale heterogeneous e-commerce network on Alibaba’s platform, crafted around a real-world risk detection scenario, and consists of diverse anonymized entities such as items, buyers, and sellers, as well as diverse transaction relations. Malicious items deliberately disguise risk information to avoid platform detection, such as by establishing "innocent" relationships with non-risk commodities, thus leading to high heterophily.

2.1.3 Finance

Motivation. Fraud detection is crucial in digital finance, a sector increasingly threatened by sophisticated fraudulent activities. Many current financial datasets [59, 3, 4] are provided in tabular form, consisting of financial transactions between accounts, which predominantly only feature homogeneous entities and relations [30]. This homogeneity limits their effectiveness in capturing the complex, multifaceted nature of financial fraud. We therefore construct the heterogeneous and heterophilic IEEE-CIS-G dataset to model a complex financial ecosystem.

Tasks. The primary task for the IEEE-CIS-G dataset is the identification of fraudulent credit card transactions through finding patterns that differentiate fraud from legitimate activity.

Dataset Construction. Developed from the Kaggle tabular dataset [26], our new IEEE-CIS-G network enhances this data by structuring it into a graph format encompassing 12 distinct types of entities, including the credit card transaction nodes and various transaction-associated entities such as payment cards and purchased products, and 22 types of relationships, effectively mirroring the complex interactions within financial transactions. Fraudulent transactions are rare and often cleverly camouflaged among a vast number of legitimate transactions, thereby creating high heterophily.

2.1.4 Social Science

Motivation. Social networks encapsulate real-world social structures and interactions, essential for analyzing social dynamics and influence patterns [35, 6, 56]. Current social network datasets, including the Facebook, Twitter, and Pokec datasets [36], predominantly feature homogeneous entities and relations, focusing solely on friendship links. To provide a more accurate representation of real-world social structure, there is a need to construct a dataset that models the rich and multifaceted nature of social interactions that are influenced by a variety of personal attributes and affiliations.

Tasks. Our new dataset H-Pokec focuses on predicting user demographic attributes, such as gender, by using social connections and personal interests, such as movies, music, and hobby groups.

Dataset Construction. To construct H-Pokec, we redefined the existing Pokec social network structure [61] by integrating directed friendship relations with edges that represent users’ affiliations in hobby groups. This approach enriches the graph with heterogeneity. Furthermore, users have some preference for friends of other demographics, such as gender, which creates heterophily.

Table 1: Statistics of \mathcal{H}^2 GB datasets. #C is the number of classes. Imbalance ratios are listed for binary classes.

Dataset	# Nodes (types)	# Edges (types)	# Features	# C (Ratio)	Label	MLH	\mathcal{H}^2 (ours)	Split Scheme (Ratio [%])	Metric
ogbn-mag	1,939,743 (4)	42,182,144 (7)	128	349	paper venue	0.8731	0.8773	Time (85/9/6)	Accuracy
mag-year	1,939,743 (4)	42,182,144 (7)	128	5	publication year	0.7718	0.9654	Random (50/25/25)	Accuracy
oag-cs	1,112,691 (4)	27,537,448 (22)	768	3,514	paper venue	0.9623	0.9652	Time (80/9/11)	Accuracy
oag-eng	929,315 (4)	12,346,854 (22)	768	3,956	paper venue	0.8689	0.8729	Time (88/10/2)	Accuracy
oag-chem	1,918,881 (4)	38,098,014 (22)	768	2,985	paper venue	0.8724	0.8858	Time (90/8/2)	Accuracy
RCDD	13,806,619 (7)	157,814,864 (14)	256	2 (11:1)	risk commodity	0.4912	0.9776	Time (70/15/15)	F1 score
IEEE-CIS-G	153,880 (12)	2,873,472 (22)	4823	2 (12:1)	fraud transaction	0.1352	0.9846	Time (80/10/10)	F1 score
H-Pokec	1,731,977 (16)	51,774,836 (31)	66	2 (1:1)	gender	0.3922	0.9488	Random (50/25/25)	Accuracy
PDNS	1,173,558 (2)	76,797,104 (4)	10	2 (1:2)	malicious domain	0.3916	0.7866	Time (70/20/10)	F1 score

2.1.5 Cybersecurity

Motivation. In the realm of cybersecurity, protecting digital infrastructure from malicious activities is important [23, 67]. The PDNS dataset models the detection of malicious DNS activities using diverse entities and relationships, which are pivotal in preempting and mitigating cyber attacks.

Tasks. The task associated with the PDNS dataset is to detect malicious DNS activity by classifying network domain nodes as either benign or malicious based on their activity patterns and associations.

Dataset Construction. PDNS, a collected dataset from [34], includes diverse entities, such as domain names and IP addresses, each representing different aspects of Internet communication. Malicious domain nodes often interact with benign domains to initiate cyber attacks, and leads to heterophily.

2.2 Class-Adjusted Heterogeneous Heterophily Index (\mathcal{H}^2 Index)

Graph heterophily is measured by the dissimilarity between two connected nodes with respect to node attributes/labels, with typical metrics such as edge heterophily [83] and node heterophily [52] that are designed for homogeneous graphs, quantifying the proportion of connected nodes with different labels. We present these standard measures for each proposed dataset in Appendix D.3. However, we observe that the current measures are problematic when directly applied to heterogeneous graphs, where relationships are not limited to direct edges between labeled task entities (e.g., "paper→paper") and can include complex metapaths² (e.g., "paper→author→paper") connecting different types of nodes. This limitation underscores the need for a better heterophily measure on heterogeneous graphs. Recent works [42, 21] have proposed the metapath-based label heterophily (MLH) measure, which extends edge heterophily [83] to a metapath-induced subgraph $\mathcal{G}_{\mathcal{P}}$.² MLH is formulated as follow, where $\mathcal{H}_{\text{edge}}$ is the edge heterophily, \mathcal{M}_k is a k -hop metapath set, and $\text{Agg} \in \{\text{mean}, \text{max}\}$ is aggregation function.

$$\text{MLH}(\mathcal{G}) = \text{Agg}(\mathcal{H}_{\text{edge}}(\mathcal{G}_{\mathcal{P}}) | \mathcal{P} \in \mathcal{M}_k), \quad \mathcal{H}_{\text{edge}}(\mathcal{G}_{\mathcal{P}}) = \frac{|\{(u, v) \in \mathcal{E} : y_u \neq y_v\}|}{|\mathcal{E}|} \quad (1)$$

However, these measurements suffer from class imbalance [41], leading to artificially low values in datasets that are inherently heterophilic. For instance, as shown in Table 1, the RCDD and IEEE-CIS-G datasets demonstrate significant class imbalance, which contributes to deceptively low MLH indices. This discrepancy arises because rare malicious nodes in these datasets are often hidden among a large majority of innocent nodes, creating a high degree of heterophily that the current measurements fail to accurately capture. Inspired by the adjusted homophily index [53, 60], we propose the *class-adjusted heterogeneous heterophily index* \mathcal{H}^2 , which can be formulated as follows.

$$\mathcal{H}^2(\mathcal{G}) = \text{Agg}(\mathcal{H}_{\text{adj}}(\mathcal{G}_{\mathcal{P}}) | \mathcal{P} \in \mathcal{M}_k), \quad \mathcal{H}_{\text{adj}}(\mathcal{G}_{\mathcal{P}}) = 1 - \frac{1 - \sum_{k=1}^C D_k^2 / (2|\mathcal{E}|)^2 - \mathcal{H}_{\text{edge}}}{1 - \sum_{k=1}^C D_k^2 / (2|\mathcal{E}|)^2}, \quad (2)$$

where $\mathcal{G}_{\mathcal{P}}$ denotes a metapath-induced subgraph², C denotes the number of classes, $d(v)$ is the in-degree of node v , $D_k = \sum_{v: y_v = k} d(v)$ is the total in-degree of class k nodes, $\mathcal{H}_{\text{edge}}$ is the edge heterophily, \mathcal{M}_k is a k -hop metapath set, and $\text{Agg} \in \{\text{mean}, \text{max}\}$ is an aggregation function. Intuitively, the adjusted heterophily \mathcal{H}_{adj} quantifies the degree of heterophily relative to what would be expected in a random graph. Under the random graph configuration model described in [49], where for every node v we create $d(v)$ copies of it and then find a random matching among all nodes, the likelihood of a given edge endpoint connecting to a node of class k is approximately $D_k / (2|\mathcal{E}|)$ (as is assumed in [53]). Thus, the expected heterophily is the likelihood that two edge endpoints are in different classes, which is $1 - \sum_{k=1}^C D_k(D_k - 1) / ((2|\mathcal{E}|)(2|\mathcal{E}| - 1)) \approx 1 - \sum_{k=1}^C D_k^2 / (2|\mathcal{E}|)^2$. As the result, a value of \mathcal{H}^2 close to 0 indicates that nodes predominantly connect to other nodes of the same class, exhibiting homophily. A value approaching or exceeding 1 suggests that nodes are more likely to connect to nodes of different classes, demonstrating heterophily. The set of all possible metapaths \mathcal{P} can potentially be large, so we introduce an additional constraint where only

²We provide the definition of metapath and metapath-induced subgraph in Appendix B.

Table 2: Different components of the state-of-the-art GT methods and components supported by our UNIFIEDGT framework. We list various representative existing GT methods that can be expressed by our framework. We omit the multi-head attention for simplicity. $\sigma(\cdot)$ denotes the softmax function. \mathbf{A} is the adjacency matrix.

Graph Type	Methods	Sampling/ Tokenization	Graph Encoding	Attention	Masking	FFN
Homogeneous Homophilic	GraphTrans [69]	—	$\mathbf{H} = \mathbf{X} \parallel \text{GNN}(\mathbf{X}, \mathbf{A})$	$\sigma\left(\frac{\mathbf{Q}\mathbf{K}^T}{\sqrt{d}}\right) \mathbf{V}$	—	$\mathbf{H} = \text{ReLU}(\mathbf{H}\mathbf{W}_1)\mathbf{W}_2$
	Gophormer [80]	Neighbor	—	$\sigma\left(\frac{\mathbf{Q}\mathbf{K}^T}{\sqrt{d}} + \phi_{ij}\mathbf{b}\right) \mathbf{V}$	\mathbf{A}_{ij}^m	$\mathbf{H} = \text{ReLU}(\mathbf{H}\mathbf{W}_1)\mathbf{W}_2$
	Graphormer [74]	—	$\mathbf{H} = \mathbf{X} + \mathbf{Z}_{\text{deg}}$	$\sigma\left(\frac{\mathbf{Q}\mathbf{K}^T}{\sqrt{d}} + \mathbf{b}_{D(i,j)}\right) \mathbf{V}$	—	$\mathbf{H} = \text{ReLU}(\mathbf{H}\mathbf{W}_1)\mathbf{W}_2$
	GraphGPS [54]	—	$\mathbf{H} = \mathbf{X} \parallel \mathbf{P}$	$\sigma\left(\frac{\mathbf{Q}\mathbf{K}^T}{\sqrt{d}}\right) \mathbf{V} + \text{GNN}(\mathbf{X}, \mathbf{A})$	—	$\mathbf{H} = \text{ReLU}(\mathbf{H}\mathbf{W}_1)\mathbf{W}_2$
	NAGphormer [9]	Hop2Seq	—	$\sigma\left(\frac{\mathbf{Q}\mathbf{K}^T}{\sqrt{d}}\right) \mathbf{V}$	—	$\mathbf{H} = \text{ReLU}(\mathbf{H}\mathbf{W}_1)\mathbf{W}_2$
Homogeneous Heterophilic	GOAT [33]	Neighbor	$\mathbf{H} = \mathbf{X} \parallel \mathbf{P}_{\text{node2vec}}$	$\sigma\left(\frac{\mathbf{Q}\mathbf{K}^T}{\sqrt{d}} + \mathbf{b}_{D(i,j)}\right) \mathbf{V}$	—	$\mathbf{H} = \text{ReLU}(\mathbf{H}\mathbf{W}_1)\mathbf{W}_2$
Heterogeneous Homophilic	HGT [29]	HGSampling	—	$\sigma\left(\frac{\mu\mathbf{Q}_{\tau(s)}\mathbf{W}_{\phi(e)}^{\text{ATT}}\mathbf{K}_{\tau(e)}^T}{\sqrt{d}}\right) \mathbf{V}_{\tau(s)}\mathbf{W}_{\phi(e)}^{\text{MSG}}$	$\mathbf{A}_{ij}^{\phi(e)}$	—
	SHGN [45]	—	—	$\sigma\left(\mathbf{a}^T [\mathbf{W}\mathbf{h}_i \parallel \mathbf{W}\mathbf{h}_j \parallel \mathbf{W}_{\tau}\mathbf{r}_{\phi(e)}]\right) \mathbf{h}_j$	\mathbf{A}_{ij}	—
	HINormer [46]	Neighbor	$\mathbf{H} = \text{GNN}(\mathbf{X}, \mathbf{A})$	$\sigma\left(\mathbf{a}^T \mathbf{W} [\mathbf{h}_i \parallel \mathbf{h}_j] + \beta \mathbf{k}_i^R \mathbf{q}_j^R\right) \mathbf{h}_j$	—	—
Heterogeneous Heterophilic	$\mathcal{H}^2\text{G-former}$ (ours)	HGSampling	$\mathbf{H}_{\tau} = \mathbf{W}_{\tau}\mathbf{X}_{\tau} \parallel \mathbf{P}_{\tau}$	$\sigma\left(\frac{\mathbf{q}_i\mathbf{W}_{\phi(e)}^{\text{MSG}}\mathbf{k}_j^T}{\sqrt{d_k}}\right) \mathbf{v}_j$	\mathbf{A}_{ij}	$\mathbf{H}_{\tau} = \text{ReLU}(\mathbf{H}_{\tau}\mathbf{W}_{\tau_1})\mathbf{W}_{\tau_2}$

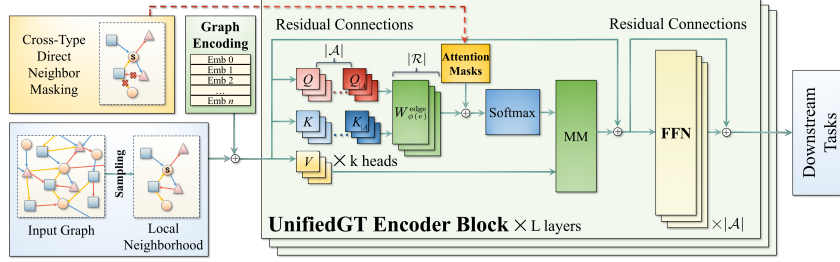


Figure 3: Overall UNIFIEDGT framework. MM stands for matrix multiplication; FFN stands for feed-forward networks; $|\mathcal{A}|$ and $|\mathcal{R}|$ are the number of node and edge types, respectively.

length-2 metapaths are considered. We select the mean function as the aggregation function to reflect the general heterophily across all metapaths. \mathcal{H}^2 is presented for each dataset in Table 1.

3 Unified Graph Transformer Framework (UNIFIEDGT)

Graph transformers excel by dynamically learning from and adapting to graph data, offering improvements that traditional GNNs struggle with. In this section, we introduce UNIFIEDGT, a modular framework that is able to encompass many existing graph transformer models and is extensible to new model designs and diverse graph tasks. By incorporating new components into UNIFIEDGT, we develop a new GT variant, $\mathcal{H}^2\text{G-former}$, to effectively handle graph heterophily and heterogeneity.

3.1 Overall Framework of UNIFIEDGT

The definition and notations for graph transformers are provided in Appendix B. As shown in Figure 3, by unifying existing graph transformer methods, we propose a general framework, UNIFIEDGT, which consists of five modular ingredients: (1) graph sampling, (2) graph encoding, (3) graph attention, (4) attention masking, and (5) feedforward networks (FFNs). The workflow of UNIFIEDGT begins with the (1) *graph sampling*, which samples a subgraph centered around the target nodes, capturing their local neighborhood. Subsequently, the (2) *graph encoding* constructs a hidden feature matrix $\mathbf{H} = [\mathbf{h}_1^T, \mathbf{h}_2^T, \dots, \mathbf{h}_n^T]^T \in \mathbb{R}^{n \times d}$, where d represents the hidden dimensionality, and $\mathbf{h}_i \in \mathbb{R}^d$ denotes the hidden feature of node i . This step projects each node feature \mathbf{x}_i through a type-specific feature projection, which is then concatenated with a structure-aware graph encoding as $\mathbf{h}_i = \mathbf{W}_{\tau(i)}\mathbf{x}_i \parallel \mathbf{P}_i$. This process effectively aligns the features from various node types into a cohesive feature space. After encoding, \mathbf{H} is processed by (3) *graph attention* and the (4) *attention masking*, where the graph structure is leveraged to refine the node features based on neighborhood context. The enhanced features are then fed to the (5) *FFNs*. The refined feature matrix \mathbf{H} can then be used for downstream tasks such as node classification or link prediction. Following established workflow, our framework is not only able to implement numerous existing GTs, as detailed in Table 2, but also enables the customization of each modular component to meet specific needs.

To deal with graphs with both heterophily and heterogeneity, we introduce a new model variant, $\mathcal{H}^2\text{G}$ -former (see Table 2). This variant augments the framework and introduces several new ingredients for components (2), (3), and (5). These enhancements include masked label embedding, cross-type heterogeneous attention, and type-specific feedforward networks (FFNs), respectively.

3.2 Modular Ingredients

Graph Sampling. Graph sampling and minibatch training are crucial for processing large-scale graphs. To extend to large graphs proposed in $\mathcal{H}^2\text{GB}$, we provide three standard sampling options: *neighbor sampling* [22], *GraphSAINT sampling* [76], and *HGSampling* [29]. Among them, neighbor sampling and HGSampling are applicable to both homogeneous and heterogeneous graphs.

Graph Encoding. Capturing the graph structure information is important for graph learning. We provide the following graph encoding options that help encode graph structure information: *Node2Vec embedding* [20], *Metapath2Vec embedding* [12], and *knowledge graph embedding* [8, 62, 71]. Furthermore, to tackle the challenges of graph heterophily, we introduce a *masked label embedding* to improve the model’s capability to understand node labels. Through a linear projection, the one-hot label vectors \mathbf{Y} extract the label embedding $\mathbf{P}_{\text{label}} = \mathbf{W}_y \mathbf{Y}$ and concatenate it to the input node features. To avoid information leakage, a portion of node labels are randomly masked during training to force the model to learn to reconstruct the node labels, similar to [24, 39].

Graph Attention. Existing GTs have predominantly been applied to homogeneous graphs, where the attention is calculated by pairwise dot products [63]. We call this *Plain Attention*. To generalize GTs to heterogeneous graphs, the diverse semantics of nodes and edges need to be considered. We introduce the design of *Cross-Type Heterogeneous Attention* that utilizes the node and edge types, as shown in Table 2. Cross-type heterogeneous attention performs type-dependent key-, query- and value-projections to model the complex connections between node types. Concretely, the projection matrices $\mathbf{W}_{K_{\tau(v)}}$, $\mathbf{W}_{Q_{\tau(v)}}$, and $\mathbf{W}_{V_{\tau(v)}}$ are applied on node v with type $\tau(v)$, to generate the corresponding \mathbf{Q} , \mathbf{K} , and \mathbf{V} matrices (Equation (3)). Furthermore, to incorporate edge type information, we design an edge-type dependent transformation $\mathbf{W}_{\phi(e)}^{\text{edge}}$ to allow modeling of diverse relations.

$$\mathbf{O} = [\mathbf{o}_1^T, \dots, \mathbf{o}_n^T]^T = \left[\left(\mathbf{h}_1 \mathbf{W}_{O_{\tau(1)}} \right)^T, \dots, \left(\mathbf{h}_n \mathbf{W}_{O_{\tau(n)}} \right)^T \right]^T, \text{ where } \mathbf{O} \in \{\mathbf{Q}, \mathbf{K}, \mathbf{V}\} \quad (3)$$

Note that typical heterogeneous GNNs only pass messages through specified meta-relations [57, 29], while our proposed heterogeneous attention mechanism enables a single node to communicate with other nodes of different types simultaneously.

Attention Masking. Existing GTs incorporate attention masking to reinforce graph inductive bias, but only allow attention to be calculated on each meta-relation separately in the heterogeneous settings [29]. We propose a new design for learning heterogeneous graph structure, *Cross-Type Attention Masking*. The attention masking (or bias) mechanism [13, 47] is shown in Equation (4), where $\mathbf{S} \in \mathbb{R}^{n \times n}$ is the attention score matrix and \mathbf{S}_{ij} represents the attention score between node pair (i, j) . The added bias is passed through the softmax function to generate an attention score (see Figure 3 and Appendix B, Equation (6)). When $-\infty$ is added to \mathbf{S}_{ij} , it essentially acts as an attention mask and zeroes out the corresponding attention scores. The *cross-type attention mask* allows a node to attend to any of its neighbors simultaneously regardless of their type.

$$\mathbf{S} = \mathbf{Q}\mathbf{K}^T / \sqrt{d_k} + \mathbf{B}, \text{ where } \mathbf{B}_{ij} = \begin{cases} 0, & \text{if } (i, j) \text{ is an edge,} \\ -\infty, & \text{otherwise.} \end{cases} \quad (4)$$

With this simple extension to the attention masking (bias) component, UNIFIEDGT is capable of expressing graph transformers with attention bias [80, 74, 33]. The HGT model [29] can also be expressed in the UNIFIEDGT when only allowing the attention scores to be calculated on meta-relations.

Type-specific FFNs. The feed-forward network (FFN) is a typical component of transformer architectures [63] that can help the model capture more complex patterns and relationships in graphs. We introduce a *type-specific FFNs* that apply dedicated FFN layers to each node type. This approach is designed to accommodate data heterogeneity, allowing the modeling of richer relationships in the semantic spaces of individual node types (Table 2).

4 Experiments

In this section, we conduct comprehensive experiments to evaluate existing and proposed methods in $\mathcal{H}^2\text{GB}$ using an Nvidia V100 GPU with 32GB of memory. All of the existing methods are

Table 3: Benchmark results of various GNN methods. Standard deviations are calculated over 5 runs with different random seeds. We highlight the **first** and **second** best results. Out-of-memory (OOM) indicates the method ran out of memory on an Nvidia V100 GPU with 32GB of memory.

	Datasets→ Methods↓	Avg. Rank	Accuracy						F1 score		
			ogbn-mag	mag-year	ogbn-cs	ogbn-eng	ogbn-chem	H-Pokec	RCDD	IEEE-CIS-G	PDNS
	MLP	22.3	27.27 ± 0.50	26.52 ± 0.64	09.26 ± 0.51	20.18 ± 0.92	13.61 ± 0.41	62.75 ± 0.34	75.87 ± 1.38	04.26 ± 8.52	73.92 ± 0.66
Graph Only	LP+1Hop	18.3	38.36	26.61 ± 0.11	19.79	36.07	22.48	45.42 ± 0.09	67.07	0.00	81.53
	LP+2Hop	14.4	37.38	39.45 ± 0.12	20.98	36.73	21.54	76.72 ± 0.07	67.84	0.00	82.13
	SGC+1Hop	23.4	16.46 ± 0.24	26.48 ± 0.17	06.42 ± 0.17	10.93 ± 3.18	07.02 ± 1.72	52.91 ± 0.43	05.47 ± 6.92	13.04 ± 3.53	74.24 ± 1.90
	SGC+2Hop	24.2	14.28 ± 0.28	26.46 ± 0.05	06.09 ± 0.50	08.77 ± 1.22	05.00 ± 1.10	59.55 ± 1.75	06.07 ± 5.29	7.98 ± 8.54	61.34 ± 1.14
Homogeneous Homophilic	GCN	14.1	42.90 ± 0.50	32.91 ± 0.50	18.22 ± 0.60	29.09 ± 0.52	18.57 ± 1.06	70.63 ± 0.36	85.81 ± 0.87	28.79 ± 1.07	81.22 ± 0.30
	GraphSAGE	8.3	40.80 ± 0.56	36.28 ± 0.19	22.92 ± 0.29	36.16 ± 0.20	24.66 ± 0.48	77.29 ± 0.30	85.02 ± 0.83	31.49 ± 1.23	91.44 ± 0.32
	GAT	11.4	48.60 ± 0.29	33.50 ± 0.62	19.12 ± 0.25	28.74 ± 0.60	14.05 ± 0.44	70.89 ± 0.20	86.71 ± 1.27	28.51 ± 0.45	93.97 ± 0.27
	GIN	15.4	37.32 ± 0.33	31.15 ± 0.54	16.33 ± 1.34	29.62 ± 1.15	17.86 ± 0.62	74.72 ± 0.32	84.22 ± 0.34	28.53 ± 0.54	87.91 ± 0.46
	APPNP	18.3	37.64 ± 0.31	29.79 ± 0.61	17.90 ± 0.60	28.63 ± 0.40	17.19 ± 1.06	57.27 ± 1.22	82.95 ± 0.67	13.64 ± 15.77	80.70 ± 0.73
	NAGphormer	11.9	42.47 ± 0.74	32.60 ± 0.06	16.49 ± 0.55	31.85 ± 0.80	23.78 ± 0.35	80.59 ± 0.15	85.46 ± 0.50	08.59 ± 9.92	92.37 ± 0.22
	GraphTrans	13.2	47.25 ± 1.54	36.14 ± 0.41	02.39 ± 0.22	6.55 ± 3.53	2.23 ± 0.2	77.8 ± 0.17	86.00 ± 0.56	30.53 ± 1.6	93.00 ± 0.39
	Gophormer	16.0	42.87 ± 0.64	35.17 ± 0.27	03.68 ± 1.24	10.42 ± 3.73	04.26 ± 2.85	71.55 ± 2.04	80.56 ± 6.13	30.79 ± 1.06	91.58 ± 0.05
Homogeneous Heterophilic	MixHop	6.3	46.99 ± 0.41	36.36 ± 0.28	23.04 ± 0.24	36.88 ± 0.73	25.03 ± 0.90	78.78 ± 0.27	85.43 ± 1.22	30.13 ± 0.86	92.78 ± 0.18
	LINKX	11.8	40.83 ± 0.18	42.81 ± 0.14	15.32 ± 0.08	32.85 ± 0.38	22.98 ± 0.24	79.66 ± 0.94	OOM	31.42 ± 1.20	87.74 ± 0.52
	FAGCN	20.0	33.06 ± 0.59	27.10 ± 0.66	10.46 ± 0.44	22.75 ± 0.94	13.01 ± 0.44	67.15 ± 0.09	81.06 ± 1.24	10.09 ± 5.09	82.84 ± 1.07
	ACM-GCN	20.1	33.50 ± 1.13	23.20 ± 1.21	11.23 ± 0.75	22.27 ± 0.77	13.81 ± 0.43	66.69 ± 0.09	75.52 ± 1.74	16.98 ± 0.29	88.48 ± 0.48
	LSGNN	13.1	38.87 ± 0.83	40.47 ± 0.58	15.20 ± 0.60	29.43 ± 0.74	19.96 ± 0.69	78.37 ± 0.49	83.84 ± 0.91	14.68 ± 1.86	88.91 ± 0.17
	GOAT	10.2	41.59 ± 0.09	32.92 ± 0.41	20.74 ± 0.39	35.82 ± 0.52	21.75 ± 0.17	76.55 ± 0.71	87.13 ± 0.45	30.31 ± 0.73	91.71 ± 0.27
Heterogeneous Homophilic	R-GCN	5.2	46.93 ± 0.46	35.60 ± 0.48	23.10 ± 1.09	37.10 ± 0.49	25.80 ± 0.32	78.05 ± 0.28	87.00 ± 1.35	31.44 ± 0.96	92.55 ± 0.44
	R-GraphSAGE	5.9	50.94 ± 0.44	38.07 ± 0.041	22.81 ± 0.63	36.11 ± 0.45	26.00 ± 0.59	77.00 ± 0.32	86.81 ± 1.74	29.85 ± 0.47	92.81 ± 0.37
	R-GAT	10.6	41.51 ± 0.47	35.40 ± 0.88	21.03 ± 0.59	35.90 ± 0.60	26.14 ± 0.34	67.17 ± 0.24	80.37 ± 0.62	22.09 ± 0.94	94.29 ± 0.16
	HAN	18.6	39.00 ± 0.22	29.66 ± 0.43	13.14 ± 1.96	27.81 ± 0.69	17.03 ± 0.66	54.04 ± 2.17	78.56 ± 1.42	23.15 ± 0.43	84.58 ± 0.76
	HGT	5.8	50.23 ± 0.48	39.47 ± 1.66	22.51 ± 0.40	35.51 ± 0.52	25.48 ± 0.76	78.91 ± 0.43	86.05 ± 1.01	30.89 ± 0.8	92.76 ± 0.15
	SHGN	10.8	43.39 ± 0.28	34.43 ± 1.23	22.03 ± 0.46	36.93 ± 0.67	24.07 ± 0.94	50.5 ± 0.89	79.67 ± 2.53	31.66 ± 0.86	89.33 ± 0.21
	\mathcal{H}^2 G-former	1.0	55.67 ± 0.35	52.55 ± 0.66	28.47 ± 0.93	46.63 ± 0.65	30.62 ± 0.31	82.45 ± 0.19	87.35 ± 0.8	31.77 ± 0.92	96.43 ± 0.21

implemented in UNIFIEDGT, and the homogeneous methods ignore the node and edge types. We demonstrate that our \mathcal{H}^2 G-former model matches or outperforms all other methods.

4.1 General Setup

Methods. We compare \mathcal{H}^2 G-former with simple baselines and three categories of state-of-art GNN and GT models, which are described in Table 2. The simple baselines include models that only consider node features, such as MLP [18], and models only consider graph topology, such as label propagation (one and two hops) [82, 51], as well as a simple GNN model that focuses on aggregation of neighborhood information with reduced nonlinearities and weight matrices, SGC [68]. The first class of GNN baselines, designed for *homogeneous homophilic* graphs, includes GCN [32], GraphSAGE [22], GAT [64], GIN [70], APPNP [16], NAGphormer [9], GraphTrans [69], and Gophormer [80]. The second class of baselines, optimized for *homogeneous heterophilic* graphs, includes MixHop [1], LINKX [41], FAGCN [7], ACM-GCN [44], LSGNN [10], and GOAT [33]. The third class of baselines, designed for *heterogeneous homophilic* graphs, includes relational GCN (R-GCN) [57], GraphSAGE (R-GraphSAGE), GAT (R-GAT), HAN [66], HGT [29], HINormer [46], and SHGN [45]. Lastly, our \mathcal{H}^2 G-former is designed for *heterogeneous heterophilic* graphs. Note that HINormer runs out of memory on every dataset and is not reported in Table 3. The detailed descriptions of each model can be found in Appendix E.1.

Training and Evaluation. The dataset splits can be found at Table 1, where most of the split strategy is based on timestamps on the nodes. Test performance is reported for the learned parameters corresponding to the highest validation performance. We use F1 score as the metric for the datasets with large class imbalance, as it is less sensitive to class imbalance than accuracy. For other datasets, we use classification accuracy as metric.

4.2 Experimental Results

Table 3 lists the results of each method across the datasets proposed in \mathcal{H}^2 GB. We make the following observations. First, \mathcal{H}^2 G-former consistently outperforms or matches the existing methods on all of the datasets. This validates the efficacy of \mathcal{H}^2 G-former as a comprehensive solution for handling graphs with heterophily and heterogeneity. Second, although homogeneous heterophilic GNNs (e.g., MixHop and GOAT) are often shown to outperform homogeneous homophilic GNNs and achieve a better average rank, their advantage diminishes when compared to heterogeneous homophilic GNNs. This performance degradation primarily stems from their inability to effectively incorporate diverse node types, edge types, and relational dynamics. As a concrete example, the semantic

meaning of each type of node can be different, resulting in different distributions in the node features. These homogeneous heterophilic GNNs cannot adjust their parameters to learn from node features of different distributions. Third, although heterogeneous homophilic GNNs are shown to have performance advantages over homogeneous heterophilic GNNs, the performance across different heterogeneous models varies significantly. This could be ascribed to their different mechanisms for handling graph heterophily. For example, models that rely on local attention mechanisms (e.g., R-GAT, HAN, and SHGN) generally perform worse. Lastly, there is a large margin between the best and worst performance in the category of homogeneous heterophilic GNNs. Many of these GNNs are generally designed for relatively small graphs and full graph training. We applied a mini-batching strategy to avoid running out of memory, but this can degrade the model performance, as also shown in [41]. This underscores the need to develop scalable GNNs that can handle graph heterophily.

5 Related Work

Graph Learning for Heterogeneous and Heterophilic Graphs. Heterogeneous GNNs are classified into *metapath-based* methods, which extract structural information from homogeneously-typed subgraphs defined by semantic paths to capture diverse semantic data [57, 77, 66, 15], and *metapath-free* methods, which process structural and semantic information simultaneously, enhancing message aggregation by incorporating node and edge types without relying on predefined paths [85, 25, 29, 45]. While these approaches take heterogeneity into account, they generally maintain the homophily assumption. In contrast, existing heterophilic GNNs have been tailored primarily for homogeneous graphs and lack mechanisms to address heterogeneity [1, 7, 41]. Recent works aim to bridge this gap by improving heterophilic learning on heterogeneous graphs through augmented graphs and disentangled loss functions [21, 38]; however, they primarily focus on enhancing existing models rather than introducing fundamentally new solutions optimized for both heterophily and heterogeneity.

Graph Transformers. Graph transformers [74, 48, 54, 79, 54, 29, 73, 33] extend to graphs the capabilities of conventional transformer architectures, which have made significant strides in nature language processing and computer vision. Transformers overcome limitations in traditional message passing GNNs [32, 22], such as over-smoothing and over-squashing [58]. Current research on graph transformers primarily focuses on homogeneous graphs [74, 33] or specialized applications like heterogeneous molecule graphs [29, 66, 54]. Our work aims to bridge this gap by providing a graph transformer framework that can handle graphs that are both heterophilic and heterogeneous.

Current Datasets. Recent evaluations of heterophilic graph learning primarily use small-scale datasets from Pei et al. [52]. Lim et al. [41] have compiled larger non-homophilous graph datasets, which have become the standard for evaluating heterophilic GNNs but are limited to homogeneous graphs. Concurrently, several heterogeneous graph datasets have been introduced, including DBLP [45], ACM [45], ogbn-mag [27], MAG240M [28], and the academic networks from IGB [31]. Despite their diversity, these datasets have not been tested with GNN methods that account for graph heterophily. Moreover, the pure focus on academic networks narrows their use in addressing graph learning challenges in other domains.

6 Conclusion

We introduced the novel graph benchmark, $\mathcal{H}^2\text{GB}$, which addresses the critical need for real-world graph benchmarks that are both heterophilic and heterogeneous. To explore the performance of existing GNNs, we presented a modular framework, UNIFIEDGT, which is able to express a wide range of existing GT and GNN models. By introducing new modules, we developed $\mathcal{H}^2\text{G-former}$ to handle graphs exhibiting both heterophily and heterogeneity. Our comprehensive experiments demonstrated the effectiveness of $\mathcal{H}^2\text{G-former}$. By integrating heterophilic learning strategies with mechanisms for managing heterogeneity, $\mathcal{H}^2\text{G-former}$ sets a new standard in modern graph learning.

Acknowledgements

This research was supported by the MIT-IBM Watson AI Lab.

References

- [1] S. Abu-El-Haija, B. Perozzi, A. Kapoor, N. Alipourfard, K. Lerman, H. Harutyunyan, G. Ver Steeg, and A. Galstyan. Mixhop: Higher-order graph convolutional architectures via sparsified neighborhood mixing. In *International Conference on Machine Learning (ICML)*, pages 21–29. PMLR, 2019.

- [2] Alibaba Group. User behavior data from Taobao for recommendation, 2018. URL <https://tianchi.aliyun.com/dataset/649>. Accessed: 2024-06-04.
- [3] E. Altman. Synthesizing credit card transactions. In *Proceedings of the ACM International Conference on AI in Finance (ICAIF)*, pages 1–9, 2021.
- [4] E. Altman, J. Blanuša, L. Von Niederhäusern, B. Egressy, A. Anghel, and K. Atasu. Realistic synthetic financial transactions for anti-money laundering models. *Advances in Neural Information Processing Systems (NeurIPS)*, 36, 2024.
- [5] M. Aravind, V. Sujadevi, M. R. Krishnan, P. S. Au, S. Pal, A. Vazhayil, G. Sridharan, and P. Poornachandran. Malicious node identification for DNS data using graph convolutional networks. In *IEEE International Conference on Recent Advances and Innovations in Engineering (ICRAIE)*, volume 7, pages 104–109, 2022.
- [6] L. Backstrom, D. Huttenlocher, J. Kleinberg, and X. Lan. Group formation in large social networks: Membership, growth, and evolution. In *Proceedings of the ACM SIGKDD International Conference on Knowledge Discovery and Data Mining (KDD)*, pages 44–54, 2006.
- [7] D. Bo, X. Wang, C. Shi, and H. Shen. Beyond low-frequency information in graph convolutional networks. In *Proceedings of the AAAI Conference on Artificial Intelligence (AAAI)*, volume 35, pages 3950–3957, 2021.
- [8] A. Bordes, N. Usunier, A. Garcia-Duran, J. Weston, and O. Yakhnenko. Translating embeddings for modeling multi-relational data. *Advances in Neural Information Processing Systems (NeurIPS)*, 26, 2013.
- [9] J. Chen, K. Gao, G. Li, and K. He. NAGphormer: A tokenized graph transformer for node classification in large graphs. In *The International Conference on Learning Representations (ICLR)*, 2022.
- [10] Y. Chen, Y. Luo, J. Tang, L. Yang, S. Qiu, C. Wang, and X. Cao. LSGNN: Towards general graph neural network in node classification by local similarity. In *Proceedings of the International Joint Conference on Artificial Intelligence (IJCAI)*, pages 3550–3558, 2023.
- [11] J. Devlin, M.-W. Chang, K. Lee, and K. Toutanova. BERT: Pre-training of deep bidirectional transformers for language understanding. In *Proceedings of the Conference of the North American Chapter of the Association for Computational Linguistics: Human Language Technologies (NAACL-HLT)*, pages 4171–4186, 2019.
- [12] Y. Dong, N. V. Chawla, and A. Swami. metapath2vec: Scalable representation learning for heterogeneous networks. In *Proceedings of the ACM SIGKDD International Conference on Knowledge Discovery and Data Mining (KDD)*, pages 135–144, 2017.
- [13] V. P. Dwivedi and X. Bresson. A generalization of transformer networks to graphs. *AAAI Workshop on Deep Learning on Graphs: Methods and Applications*, 2021.
- [14] M. Fey and J. E. Lenssen. Fast graph representation learning with PyTorch Geometric. In *ICLR Workshop on Representation Learning on Graphs and Manifolds*, 2019.
- [15] X. Fu, J. Zhang, Z. Meng, and I. King. MAGNN: Metapath aggregated graph neural network for heterogeneous graph embedding. In *Proceedings of the International Conference on World Wide Web (WWW)*, pages 2331–2341, 2020.
- [16] J. Gasteiger, A. Bojchevski, and S. Günnemann. Predict then propagate: Graph neural networks meet personalized PageRank. In *International Conference on Learning Representations*, 2019.
- [17] J. Gilmer, S. S. Schoenholz, P. F. Riley, O. Vinyals, and G. E. Dahl. Neural message passing for quantum chemistry. In *International Conference on Machine Learning (ICML)*, pages 1263–1272, 2017.
- [18] I. Goodfellow, Y. Bengio, and A. Courville. *Deep Learning*. MIT Press, 2016.
- [19] J.-B. Grill, F. Strub, F. Altché, C. Tallec, P. Richemond, E. Buchatskaya, C. Doersch, B. Avila Pires, Z. Guo, M. Gheshlaghi Azar, et al. Bootstrap your own latent: A new approach to self-supervised learning. *Advances in Neural Information Processing Systems (NeurIPS)*, 33:21271–21284, 2020.
- [20] A. Grover and J. Leskovec. node2vec: Scalable feature learning for networks. In *Proceedings of the ACM SIGKDD International Conference on Knowledge Discovery and Data Mining (KDD)*, pages 855–864, 2016.

- [21] J. Guo, L. Du, W. Bi, Q. Fu, X. Ma, X. Chen, S. Han, D. Zhang, and Y. Zhang. Homophily-oriented heterogeneous graph rewiring. In *Proceedings of the International Conference on World Wide Web (WWW)*, pages 511–522, 2023.
- [22] W. Hamilton, Z. Ying, and J. Leskovec. Inductive representation learning on large graphs. *Advances in Neural Information Processing Systems (NeurIPS)*, 30, 2017.
- [23] H. He, Y. Ji, and H. H. Huang. Illuminati: Towards explaining graph neural networks for cybersecurity analysis. In *IEEE European Symposium on Security and Privacy (EuroS&P)*, pages 74–89, 2022.
- [24] K. He, X. Chen, S. Xie, Y. Li, P. Dollár, and R. Girshick. Masked autoencoders are scalable vision learners. In *Proceedings of the IEEE/CVF Conference on Computer Vision and Pattern Recognition (CVPR)*, pages 16000–16009, 2022.
- [25] H. Hong, H. Guo, Y. Lin, X. Yang, Z. Li, and J. Ye. An attention-based graph neural network for heterogeneous structural learning. In *Proceedings of the AAAI Conference on Artificial Intelligence (AAAI)*, volume 34, pages 4132–4139, 2020.
- [26] A. Howard, B. Bouchon-Meunier, I. CIS, J. Lei, Lynn@Vesta, Marcus2010, and H. Abbass. IEEE-CIS fraud detection. Kaggle, 2019. URL <https://www.kaggle.com/competitions/ieee-fraud-detection>.
- [27] W. Hu, M. Fey, M. Zitnik, Y. Dong, H. Ren, B. Liu, M. Catasta, and J. Leskovec. Open graph benchmark: Datasets for machine learning on graphs. *Advances in Neural Information Processing Systems (NeurIPS)*, 33:22118–22133, 2020.
- [28] W. Hu, M. Fey, H. Ren, M. Nakata, Y. Dong, and J. Leskovec. OGB-LSC: A large-scale challenge for machine learning on graphs. In *Advances in Neural Information Processing Systems (NeurIPS), Datasets and Benchmarks Track*, 2021.
- [29] Z. Hu, Y. Dong, K. Wang, and Y. Sun. Heterogeneous graph transformer. In *Proceedings of the International Conference on World Wide Web (WWW)*, pages 2704–2710, 2020.
- [30] X. Huang, Y. Yang, Y. Wang, C. Wang, Z. Zhang, J. Xu, L. Chen, and M. Vazirgiannis. DGraph: A large-scale financial dataset for graph anomaly detection. *Advances in Neural Information Processing Systems (NeurIPS)*, 35:22765–22777, 2022.
- [31] A. Khatua, V. S. Mailthody, B. Taleka, T. Ma, X. Song, and W.-m. Hwu. IGB: Addressing the gaps in labeling, features, heterogeneity, and size of public graph datasets for deep learning research. In *Proceedings of the ACM SIGKDD Conference on Knowledge Discovery and Data Mining (KDD)*, 2023.
- [32] T. N. Kipf and M. Welling. Semi-supervised classification with graph convolutional networks. In *International Conference on Learning Representations (ICLR)*, 2017.
- [33] K. Kong, J. Chen, J. Kirchenbauer, R. Ni, C. B. Bruss, and T. Goldstein. GOAT: A global transformer on large-scale graphs. In *Proceedings of the International Conference on Machine Learning (ICML)*, pages 17375–17390, 2023.
- [34] U. Kumarasinghe, F. Deniz, and M. Nabeel. PDNS-Net: A large heterogeneous graph benchmark dataset of network resolutions for graph learning. *arXiv preprint arXiv:2203.07969*, 2022.
- [35] J. Leskovec and J. McAuley. Learning to discover social circles in ego networks. *Advances in Neural Information Processing Systems (NeurIPS)*, 25, 2012.
- [36] J. Leskovec and R. Sosič. SNAP: A general-purpose network analysis and graph-mining library. *ACM Transactions on Intelligent Systems and Technology (TIST)*, 8(1):1–20, 2016.
- [37] J. Leskovec, L. A. Adamic, and B. A. Huberman. The dynamics of viral marketing. *ACM Transactions on the Web (TWEB)*, 1(1):5–es, 2007.
- [38] J. Li, Z. Wei, J. Dan, J. Zhou, Y. Zhu, R. Wu, B. Wang, Z. Zhen, C. Meng, H. Jin, et al. Hetero2Net: Heterophily-aware representation learning on heterogeneous graphs. *arXiv preprint arXiv:2310.11664*, 2023.
- [39] J. Li, R. Wu, W. Sun, L. Chen, S. Tian, L. Zhu, C. Meng, Z. Zheng, and W. Wang. What’s behind the mask: Understanding masked graph modeling for graph autoencoders. In *Proceedings of the ACM SIGKDD Conference on Knowledge Discovery and Data Mining (KDD)*, pages 1268–1279, 2023.
- [40] X. Li, R. Zhu, Y. Cheng, C. Shan, S. Luo, D. Li, and W. Qian. Finding global homophily in graph neural networks when meeting heterophily. In *International Conference on Machine Learning (ICML)*, pages 13242–13256, 2022.

- [41] D. Lim, F. Hohne, X. Li, S. L. Huang, V. Gupta, O. Bhalerao, and S. N. Lim. Large scale learning on non-homophilous graphs: New benchmarks and strong simple methods. *Advances in Neural Information Processing Systems (NeurIPS)*, 34:20887–20902, 2021.
- [42] Y. Liu, H. Zhang, C. Yang, A. Li, Y. Ji, L. Zhang, T. Li, J. Yang, T. Zhao, J. Yang, et al. Datasets and interfaces for benchmarking heterogeneous graph neural networks. In *Proceedings of the ACM International Conference on Information and Knowledge Management (CIKM)*, pages 5346–5350, 2023.
- [43] I. Loshchilov and F. Hutter. SGDR: Stochastic gradient descent with warm restarts. In *International Conference on Learning Representations (ICLR)*, 2017.
- [44] S. Luan, C. Hua, Q. Lu, J. Zhu, M. Zhao, S. Zhang, X.-W. Chang, and D. Precup. Revisiting heterophily for graph neural networks. *Advances in Neural Information Processing Systems (NeurIPS)*, 35:1362–1375, 2022.
- [45] Q. Lv, M. Ding, Q. Liu, Y. Chen, W. Feng, S. He, C. Zhou, J. Jiang, Y. Dong, and J. Tang. Are we really making much progress? revisiting, benchmarking and refining heterogeneous graph neural networks. In *Proceedings of the ACM SIGKDD Conference on Knowledge Discovery and Data Mining (KDD)*, pages 1150–1160, 2021.
- [46] Q. Mao, Z. Liu, C. Liu, and J. Sun. Hinormer: Representation learning on heterogeneous information networks with graph transformer. In *Proceedings of the International Conference on World Wide Web (WWW)*, pages 599–610, 2023.
- [47] G. Mialon, D. Chen, M. Selosse, and J. Mairal. Graphit: Encoding graph structure in transformers. *arXiv preprint arXiv:2106.05667*, 2021.
- [48] E. Min, R. Chen, Y. Bian, T. Xu, K. Zhao, W. Huang, P. Zhao, J. Huang, S. Ananiadou, and Y. Rong. Transformer for graphs: An overview from architecture perspective. *arXiv preprint arXiv:2202.08455*, 2022.
- [49] M. Molloy and B. A. Reed. A critical point for random graphs with a given degree sequence. *Random Structures & Algorithms*, 6:161–180, 1995.
- [50] A. Paszke, S. Gross, F. Massa, A. Lerer, J. Bradbury, G. Chanan, T. Killeen, Z. Lin, N. Gimelshein, L. Antiga, et al. PyTorch: An imperative style, high-performance deep learning library. *Advances in Neural Information Processing Systems (NeurIPS)*, 32, 2019.
- [51] L. Peel. Graph-based semi-supervised learning for relational networks. In *Proceedings of the SIAM International Conference on Data Mining (SDM)*, pages 435–443, 2017.
- [52] H. Pei, B. Wei, K. C.-C. Chang, Y. Lei, and B. Yang. Geom-GCN: Geometric graph convolutional networks. In *International Conference on Learning Representations (ICLR)*, 2020.
- [53] O. Platonov, D. Kuznedelev, A. Babenko, and L. Prokhorenkova. Characterizing graph datasets for node classification: Homophily-heterophily dichotomy and beyond. *Advances in Neural Information Processing Systems (NeurIPS)*, 36, 2024.
- [54] L. Rampášek, M. Galkin, V. P. Dwivedi, A. T. Luu, G. Wolf, and D. Beaini. Recipe for a general, powerful, scalable graph transformer. *Advances in Neural Information Processing Systems (NeurIPS)*, 35: 14501–14515, 2022.
- [55] S. X. Rao, S. Zhang, Z. Han, Z. Zhang, W. Min, Z. Chen, Y. Shan, Y. Zhao, and C. Zhang. xFraud: Explainable fraud transaction detection. *Proceedings of the VLDB Endowment (PVLDB)*, 15(3):427–436, 2021.
- [56] B. Rozemberczki and R. Sarkar. Twitch gamers: A dataset for evaluating proximity preserving and structural role-based node embeddings. *arXiv preprint arXiv:2101.03091*, 2021.
- [57] M. Schlichtkrull, T. N. Kipf, P. Bloem, R. Van Den Berg, I. Titov, and M. Welling. Modeling relational data with graph convolutional networks. In *European Semantic Web Conference (ESWC)*, pages 593–607, 2018.
- [58] Y. Song, C. Zhou, X. Wang, and Z. Lin. Ordered GNN: Ordering message passing to deal with heterophily and over-smoothing. In *International Conference on Learning Representations (ICLR)*, 2023.
- [59] M. Starnini, C. E. Tsourakakis, M. Zamanipour, A. Panisson, W. Allasia, M. Fornasiero, L. L. Puma, V. Ricci, S. Ronchiadin, A. Ugrinoska, et al. Smurf-based anti-money laundering in time-evolving transaction networks. In *European Conference on Machine Learning and Data Mining (ECML PKDD)*, pages 171–186, 2021.

- [60] S. Suresh, V. Budde, J. Neville, P. Li, and J. Ma. Breaking the limit of graph neural networks by improving the assortativity of graphs with local mixing patterns. In *Proceedings of the ACM SIGKDD Conference on Knowledge Discovery and Data Mining (KDD)*, pages 1541–1551, 2021.
- [61] L. Takac and M. Zabovsky. Data analysis in public social networks. In *International Scientific Conference and International Workshop Present Day Trends of Innovations*, volume 1, 2012.
- [62] T. Trouillon, J. Welbl, S. Riedel, É. Gaussier, and G. Bouchard. Complex embeddings for simple link prediction. In *International Conference on Machine Learning (ICML)*, pages 2071–2080, 2016.
- [63] A. Vaswani, N. Shazeer, N. Parmar, J. Uszkoreit, L. Jones, A. N. Gomez, Ł. Kaiser, and I. Polosukhin. Attention is all you need. *Advances in Neural Information Processing Systems (NeurIPS)*, 30, 2017.
- [64] P. Veličković, G. Cucurull, A. Casanova, A. Romero, P. Liò, and Y. Bengio. Graph attention networks. In *International Conference on Learning Representations (ICLR)*, 2018.
- [65] D. Wang, J. Lin, P. Cui, Q. Jia, Z. Wang, Y. Fang, Q. Yu, J. Zhou, S. Yang, and Y. Qi. A semi-supervised graph attentive network for financial fraud detection. In *IEEE International Conference on Data Mining (ICDM)*, pages 598–607, 2019.
- [66] X. Wang, H. Ji, C. Shi, B. Wang, Y. Ye, P. Cui, and P. S. Yu. Heterogeneous graph attention network. In *Proceedings of the International Conference on World Wide Web (WWW)*, pages 2022–2032, 2019.
- [67] D. Warmsley, A. Waagen, J. Xu, Z. Liu, and H. Tong. A survey of explainable graph neural networks for cyber malware analysis. In *IEEE International Conference on Big Data (Big Data)*, pages 2932–2939. IEEE, 2022.
- [68] F. Wu, A. Souza, T. Zhang, C. Fifty, T. Yu, and K. Weinberger. Simplifying graph convolutional networks. In *International Conference on Machine Learning (ICML)*, pages 6861–6871, 2019.
- [69] Z. Wu, P. Jain, M. Wright, A. Mirhoseini, J. E. Gonzalez, and I. Stoica. Representing long-range context for graph neural networks with global attention. *Advances in Neural Information Processing Systems (NeurIPS)*, 34:13266–13279, 2021.
- [70] K. Xu, W. Hu, J. Leskovec, and S. Jegelka. How powerful are graph neural networks? In *International Conference on Learning Representations (ICLR)*, 2019.
- [71] B. Yang, W.-t. Yih, X. He, J. Gao, and L. Deng. Embedding entities and relations for learning and inference in knowledge bases. In *The International Conference on Learning Representations (ICLR)*, 2015.
- [72] Z. Yang, Z. Dai, Y. Yang, J. Carbonell, R. R. Salakhutdinov, and Q. V. Le. XLNet: Generalized autoregressive pretraining for language understanding. *Advances in Neural Information Processing Systems (NeurIPS)*, 32, 2019.
- [73] S. Yao, T. Wang, and X. Wan. Heterogeneous graph transformer for graph-to-sequence learning. In *Proceedings of the Annual Meeting of the Association for Computational Linguistics (ACL)*, pages 7145–7154, 2020.
- [74] C. Ying, T. Cai, S. Luo, S. Zheng, G. Ke, D. He, Y. Shen, and T.-Y. Liu. Do transformers really perform bad for graph representation? In *Advances in Neural Information Processing Systems (NeurIPS)*, pages 28877–28888, 2021.
- [75] J. You, Z. Ying, and J. Leskovec. Design space for graph neural networks. *Advances in Neural Information Processing Systems (NeurIPS)*, 33:17009–17021, 2020.
- [76] H. Zeng, H. Zhou, A. Srivastava, R. Kannan, and V. Prasanna. GraphSAINT: Graph sampling based inductive learning method. In *International Conference on Learning Representations (ICLR)*, 2020.
- [77] C. Zhang, D. Song, C. Huang, A. Swami, and N. V. Chawla. Heterogeneous graph neural network. In *Proceedings of the ACM SIGKDD International Conference on Knowledge Discovery and Data Mining (KDD)*, pages 793–803, 2019.
- [78] F. Zhang, X. Liu, J. Tang, Y. Dong, P. Yao, J. Zhang, X. Gu, Y. Wang, B. Shao, R. Li, et al. OAG: Toward linking large-scale heterogeneous entity graphs. In *Proceedings of the ACM SIGKDD International Conference on Knowledge Discovery and Data Mining (KDD)*, pages 2585–2595, 2019.
- [79] S. Zhang, Q. Ning, and L. Huang. Extracting temporal event relation with syntax-guided graph transformer. In *North American Chapter of the Association for Computational Linguistics (NAACL)*, pages 379–390, July 2022.

- [80] J. Zhao, C. Li, Q. Wen, Y. Wang, Y. Liu, H. Sun, X. Xie, and Y. Ye. Gophormer: Ego-graph transformer for node classification. *arXiv preprint arXiv:2110.13094*, 2021.
- [81] X. Zheng, Y. Liu, S. Pan, M. Zhang, D. Jin, and P. S. Yu. Graph neural networks for graphs with heterophily: A survey. *arXiv preprint arXiv:2202.07082*, 2022.
- [82] D. Zhou, O. Bousquet, T. Lal, J. Weston, and B. Schölkopf. Learning with local and global consistency. *Advances in Neural Information Processing Systems (NeurIPS)*, 16, 2003.
- [83] J. Zhu, Y. Yan, L. Zhao, M. Heimann, L. Akoglu, and D. Koutra. Beyond homophily in graph neural networks: Current limitations and effective designs. *Advances in Neural Information Processing Systems (NeurIPS)*, 33:7793–7804, 2020.
- [84] J. Zhu, R. A. Rossi, A. Rao, T. Mai, N. Lipka, N. K. Ahmed, and D. Koutra. Graph neural networks with heterophily. In *Proceedings of the AAAI Conference on Artificial Intelligence (AAAI)*, volume 35, pages 11168–11176, 2021.
- [85] S. Zhu, C. Zhou, S. Pan, X. Zhu, and B. Wang. Relation structure-aware heterogeneous graph neural network. In *IEEE International Conference on Data Mining (ICDM)*, pages 1534–1539, 2019.

A Dataset Documentation, Metadata and Intended Use

All datasets in $\mathcal{H}^2\text{GB}$ are intended for academic use, and their corresponding licenses are described in Appendix D.1. We release our $\mathcal{H}^2\text{GB}$ as an open-source library under the [MIT license](#). We bear all responsibility in case of violation of rights. For ease of access, we provide the following links to the $\mathcal{H}^2\text{GB}$ benchmark suite and UNIFIEDGT framework.

- Open-source code and library can be found at <https://github.com/junhongmit/H2GB/>.
- $\mathcal{H}^2\text{GB}$ Python package is available via pypi at <https://pypi.org/project/H2GB/>.
- Datasets and documentation can be found at <https://junhongmit.github.io/H2GB/>.

Croissant Metadata. Croissant metadata record documenting each dataset can be found at:

- ogbn-mag, mag-year: Croissant metadata.
- oag-cs, oag-eng, oag-chem: Croissant metadata.
- RCDD: Croissant metadata.
- IEEE-CIS: Croissant metadata.
- H-Pokec: Croissant metadata.
- PDNS: Croissant metadata.

Maintenance Plan. To maintain the relevance and utility of $\mathcal{H}^2\text{GB}$, we plan to continue developing and maintaining $\mathcal{H}^2\text{GB}$ based on community feedback and evolving research needs. The $\mathcal{H}^2\text{GB}$ and its accompanying baseline implementations will be regularly updated and maintained in our dedicated GitHub repository. We plan to extend the benchmark by incorporating additional datasets, improving existing methodologies, and refining our evaluation metrics in response to new insights and advancements in the field.

B Preliminaries

Definition 1 (Graph Heterogeneity). A heterogeneous graph is defined as a directed graph $\mathcal{G} = (\mathcal{V}, \mathcal{E}, \mathcal{A}, \mathcal{R})$, where each node $v \in \mathcal{V}$ and edge $e \in \mathcal{E}$ is associated with their type mapping function $\tau(v) : \mathcal{V} \rightarrow \mathcal{A}$ and $\phi(e) : \mathcal{E} \rightarrow \mathcal{R}$, respectively. \mathcal{A} and \mathcal{R} denotes the set of node and edge types. For the node classification task, usually, only a single type of nodes (*task entity*) are tagged with labels.

Definition 2 (Metarelation). For edge $e = (s, t)$ connecting source node s to target node t , its metarelation is denoted as $\langle \tau(s), \phi(e), \tau(t) \rangle$. A metapath of length n , defined as $\mathcal{P} = A_1 \xrightarrow{R_1} A_2 \xrightarrow{R_2} \dots \xrightarrow{R_n} A_{n+1}$, is a sequence of metarelations, where $A_i \in \mathcal{A}$, $R_i \in \mathcal{R}$ for all i . For example, in an academic network, a metapath "paper \rightarrow author \rightarrow paper" represents papers written by the same author.

Definition 3 (Metapath-Induced Subgraphs). Given a metapath \mathcal{P} , we can construct the corresponding metapath-induced subgraph $\mathcal{G}_{\mathcal{P}}$, which includes edge (u, v) in $\mathcal{G}_{\mathcal{P}}$ if and only if there exists at least one length- n path between u and v following the metapath \mathcal{P} in the original graph \mathcal{G} .

Definition 4 (Graph Heterophily). Graph heterophily is measured by the dissimilarity between two connected nodes with respect to their node attributes/labels, with typical metrics such as edge heterophily [83] and node heterophily [52] that are designed for homogeneous graphs, quantifying the proportion of connected nodes that have different labels.

Graph Transformer (GT). Here, we provide a discussion of how graph transformers transform the graph representation. A transformer is a stack of alternating blocks of multi-head attention (MHA) and fully connected feed-forward networks (FFNs). Let \mathcal{G} be a graph with node feature matrix $\mathbf{X} = [\mathbf{x}_1^T, \mathbf{x}_2^T, \dots, \mathbf{x}_n^T]^T \in \mathbb{R}^{n \times d}$, where d is the hidden dimension and $\mathbf{x}_i \in \mathbb{R}^d$ is the node feature at position i . In each layer l ($l > 0$), given the hidden feature matrix $\mathbf{H}^{(l-1)} \in \mathbb{R}^{n \times d}$, where $\mathbf{H}^{(0)} = \mathbf{X}$, the MHA module first linearly projects the input $\mathbf{H}^{(l-1)}$ to the query-, key-, value-spaces, resulting in the matrices \mathbf{Q} , \mathbf{K} , and \mathbf{V} (Equation (5)). The parameter matrices are denoted by \mathbf{W}_Q , \mathbf{W}_K , and $\mathbf{W}_V \in \mathbb{R}^{d \times d_K}$.

$$\mathbf{Q} = \mathbf{H}^{(l-1)} \mathbf{W}_Q, \mathbf{K} = \mathbf{H}^{(l-1)} \mathbf{W}_K, \mathbf{V} = \mathbf{H}^{(l-1)} \mathbf{W}_V, \quad (5)$$

$$\text{MHA}(\mathbf{H}^{(l-1)}) = \text{softmax}\left(\frac{\mathbf{Q}\mathbf{K}^T}{\sqrt{d_K}}\right) \mathbf{V}, \quad (6)$$

Then, a single attention head computes the scaled dot-product as shown in Equation (6), where the softmax is applied row-wise, and d_k denotes the feature dimension of the matrices Q and K . Multi-head attention $\text{MHA}(\mathbf{H}^{(l-1)})$ concatenates several attention heads together. By combining the above with additional residual connections and normalization, the transformer layer updates features $\mathbf{H}^{(l-1)}$ through the equations

$$\hat{\mathbf{H}}^{(l)} = \text{MHA}(\mathbf{H}^{(l-1)}) + \mathbf{H}^{(l-1)} \quad (7)$$

$$\mathbf{H}^{(l)} = \text{FFN}(\hat{\mathbf{H}}^{(l)}) + \mathbf{H}^{(l)} = \left[\sigma(\hat{\mathbf{H}}^{(l)} \mathbf{W}_1) \mathbf{W}_2 \right] + \mathbf{H}^{(l)}, \quad (8)$$

where σ refers to the activation function, and $\mathbf{W}_1 \in \mathbb{R}^{d \times d_f}$, $\mathbf{W}_2 \in \mathbb{R}^{d_f \times d}$ contain trainable parameters in the feedforward network (FFN) layer. Transformers can learn the feature-based proximities between different positions for the input node feature matrix, and the final output $\mathbf{H}^{(L)} \in \mathbb{R}^{n \times d}$ can be used as the updated node representation for downstream tasks, such as node classification.

C Discussion

Societal Impact. The $\mathcal{H}^2\text{GB}$ benchmark and its associated datasets are designed to foster advancements in graph learning, particularly in contexts that feature both heterophily and heterogeneity. By integrating datasets from diverse domains such as academia, finance, e-commerce, social networks, and cybersecurity, $\mathcal{H}^2\text{GB}$ facilitates research on high-impact challenges like financial fraud detection and malware identification. The availability of such a benchmark can inspire novel methodological advancements and practical applications, potentially leading to more robust and effective solutions for real-world problems.

Potential Negative Impact. While $\mathcal{H}^2\text{GB}$ aims to standardize and enhance graph learning, its widespread adoption might inadvertently narrow the focus of future research to its specific datasets and tasks. Such a scenario could limit exploration and innovation with other graph types and learning settings. To mitigate this risk, we plan to actively engage with the research community to incorporate feedback and expand $\mathcal{H}^2\text{GB}$ regularly, introducing new datasets and challenges that reflect emerging needs.

Limitations. Currently, $\mathcal{H}^2\text{GB}$ focuses on node classification tasks. This focus is driven by the definition of heterophily in terms of node labels and mirrors the settings explored by existing studies on homogeneous heterophilic GNNs [83, 41]. While this focus aligns well with the need to understand performance under conditions of label heterophily, it does not fully exploit the potential of our datasets and framework for other types of graph learning tasks, such as link prediction. Future extensions of $\mathcal{H}^2\text{GB}$ will aim to diversify the types of supported tasks, enhancing its utility and relevance for a broader array of applications.

D Further Dataset Details

D.1 Licenses

In this section, we indicate the licenses of the datasets that we collect:

- ogbn-mag, mag-year: ODC-BY license. The dataset is downloaded from the Open Graph Benchmark [27], and the dataset is a subset of the Microsoft Academic Graph.
- oag-cs, oag-eng, oag-chem: ODC-BY license. The datasets are extracted from the Open Academic Graph (OAG), which is licensed under ODC-BY. The original OAG dataset is publicly available online here [78].
- RCDD: CC BY 4.0 license. The original dataset can be found here [42]. Due to the sensitivity of e-commerce data, for confidentiality and security purposes, except for the item type, the names of the other node types (e.g., buyer and seller) and edge types (e.g., buy and sell) are redacted and represented by letters. All of the nodes are represented by numerical IDs, and node features are only provided as numerical values.
- IEEE-CIS: The dataset is provided by IEEE Computational Intelligence Society in a Kaggle competition [26], and now is publicly available here. To the best of our knowledge, it was not released with a license. The financial transactions in this dataset are anonymized and only numerical IDs are provided.

- **Pokec:** BSD license. The dataset was retrieved from SNAP [36], and the original source of the data is from [61]. SNAP is distributed under the BSD license, which means that it is free for both academic and commercial use. Additionally, in this dataset, we only provide numerical values as node features and remove all of the raw text to de-identify personal information.
- **PDNS:** The dataset was publicly released by an arXiv paper [34], and the original dataset is available here. To the best of our knowledge, the dataset was not released with a license. The graph dataset we provided is anonymized, and only numerical IDs are provided.

D.2 Dataset Details.

The proposed datasets provided in $\mathcal{H}^2\text{GB}$ can be accessed in the widely-used heterogeneous graph data object format supported by PyTorch Geometric library (HeteroData). Further details on each dataset are provided below.

- **ogbn-mag** [27] is a heterogeneous graph composed of a subset of the Microsoft Academic Graph (MAG). It contains four types of entities—papers, authors, institutions, and field of study—as well as four types of directed relations connecting two types of entities. Each paper is associated with a 128-dimensional Word2Vec feature vector, and all of the other types of entities are originally not associated with any input node features. We average the node features of all the published papers of an author to obtain the author feature. Similarly, node features of all the affiliated authors in an institution are averaged to obtain institution features. Each paper node is labeled with its published venue. We follow the official dataset splitting, where the training set contains all papers published before 2018, and the validation and test sets contain the papers published in 2018 and since 2019, respectively.
- **mag-year** [27] is the ogbn-mag dataset with different labels. We set the paper node labels to be based on the publication year instead of the paper venue. The graph structure is exactly the same as ogbn-mag. The five classes are chosen by partitioning the publication years such that class ratios are approximately balanced.
- **oag-cs**, **oag-eng**, and **oag-chem** are new heterogeneous graphs composed of subsets of the Open Academic Graph (OAG) [78]. Each of the datasets contains papers from three different subject domains—computer science, engineering, and chemistry. These datasets also contain four types of entities—papers, authors, institutions, and fields of study. Each paper is associated with a 768-dimensional feature vector generated from a pre-trained XLNet [72] applied on the paper titles. The representation of each word in the title is weighted by the word’s attention to obtain the title representation for each paper. Each paper node is labeled with its published venue (paper or conference). We split the papers as follows: the training set consists of papers published up to 2016, the validation set contains papers published in 2017, and the test set contains papers published in 2018 and since 2019.
- **RCCD** (Risk Commodity Detection Dataset) is a large-scale heterogeneous e-commerce network extracted from Alibaba’s e-commerce platform based on a real risk detection scenario. Risk commodities always deliberately disguise risk information, for example, forging "innocent" relationships by forging devices, addresses, or other methods. For confidentiality and security, except for the item type, the names of the other node types (e.g., buyer and seller) and edge types (e.g., buy and sell) are redacted and represented by letters. Each commodity is associated with a 256-dimensional feature vector concatenated by the text and image features extracted from pre-trained models, BERT [11] and BYOL [19], respectively. Each item node is labeled with a binary label indicating whether or not is a risk commodity. We follow the official dataset splitting, where the validation set is split from the training set, and the test set is obtained over time.
- **IEEE-CIS-G** is a heterogeneous financial network extracted from a tabular transaction dataset from Kaggle [26]. The original dataset contains credit card transactions provided by Vesta Corporation, a leading payment service company whose data consists of verified transactions. We defined a bipartite graph structure, where one partition represents the credit card transaction nodes and the other partition represents the available information linked to each credit card transaction (e.g., product code, card information, purchaser and recipient email domain, etc.). The graph, therefore, contains 12 diverse entities, including the transaction nodes and transaction information nodes. It also consists of 22 types of relations, connecting a transaction node to each information node. Each transaction is associated with a 4823-dimensional feature vector extracted from the transaction’s categorical and numerical features. More description of the features can be found in the Kaggle discussion. Each transaction node is labeled with a binary label indicating whether or not it is a

fraudulent transaction. This dataset has around 4% of fraudulent transactions. We split the dataset over the timestamp of transactions.

- H-Pokec is a heterogeneous friendship graph of a Slovak online social network [61], which consists of multiple types of entities—users and different areas of hobby clubs (e.g., movies and music clubs)—as well as multiple types of directed edges representing the friendship relations and the affiliation to the hobby clubs. Each user node is associated with a 66-dimensional feature vector extracted from the user profile information, such as geographical region, age, and visibility of the user profile. Each user node is labeled with a value indicating their reported gender. This dataset is randomly split into training, validation, and test sets.
- P-DNS is a heterogeneous cybersecurity graph constructed from passive DNS data. This dataset originates from a seed set of malicious domains collected from VirusTotal, coupled with their associated hosting infrastructures derived from a comprehensive passive DNS repository that routinely logs global domain resolutions [34]. It consists of two kinds of entities, domain nodes and IP nodes, linked by four relationship types, such as "domain similarity" and "domain-to-IP resolution". Each domain node is associated with a 10-dimensional node feature vector derived from domain analysis, including the count of subdomains and indicators of brand impersonation, specifically whether the domain impersonates a popular top brand. Each domain node is labeled with a binary value indicating whether it is a malicious domain. The dataset is split temporally, with the test set defined after a specific cut-off date, ensuring that training and validation sets comprise data from earlier periods to maintain the integrity of temporal data splits.

Lastly, we present the heterogeneous graph schema for each proposed dataset in Figure 4. The schema is a specialized graph illustrating type information, where nodes represent node types, and edges indicate edge types connecting different node types. Additionally, we provide the number of each type of node and edge in the legend.

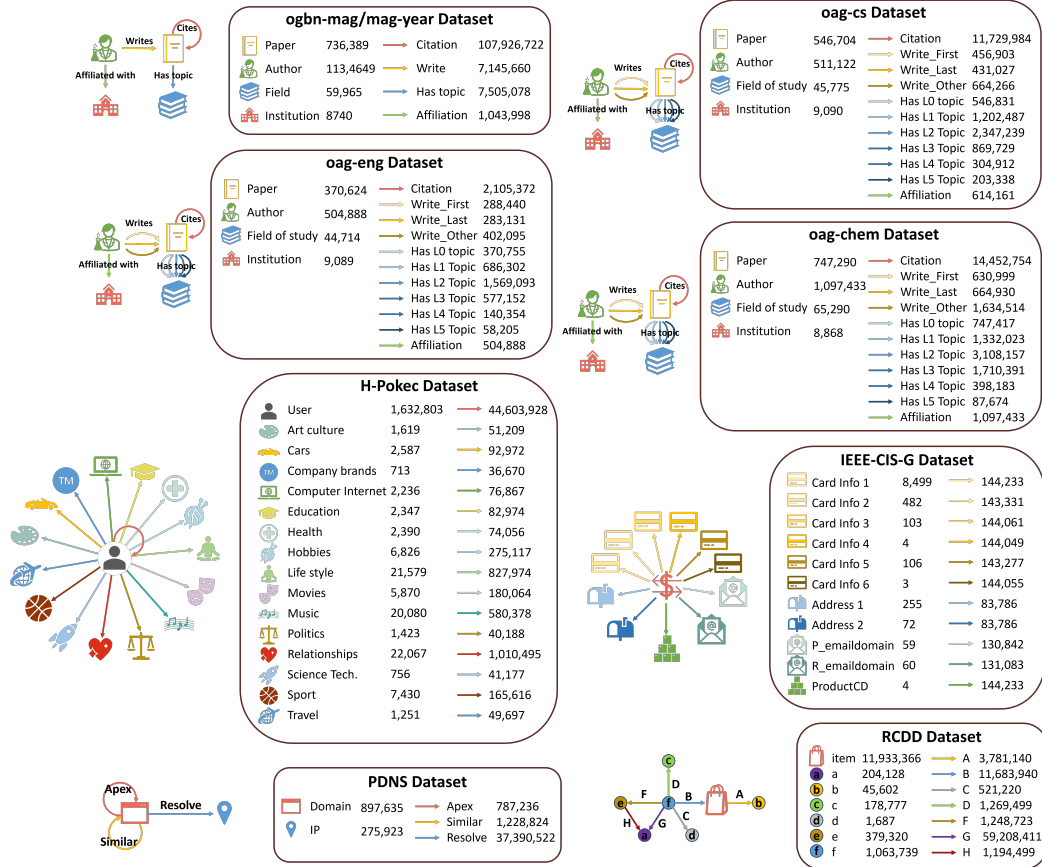


Figure 4: The schema and node/edge information of each proposed dataset.

Table 4: Existing homogeneous heterophily measures on each proposed dataset by simply ignoring the node and edge type information.

	ogbn-mag	mag-year	oag-cs	oag-eng	oag-chem	H-Pokec	RCDD	IEEE-CIS-G	PDNS
Edge Heterophily [83]	0.9205	0.7909	0.9835	0.9586	0.9457	0.5663	0.5001	0.5917	0.4990
Node Heterophily [52]	0.9539	0.7946	0.9880	0.9748	0.9696	0.5667	0.5005	0.5839	0.4992
Adjusted Heterophily [53]	0.9312	0.9977	0.9847	0.9612	0.9496	1.1350	0.8398	1.3151	1.0027

D.3 Additional Heterophily Measures

Here we present existing heterophily measures on our datasets. These measures include edge heterophily [83], node heterophily [52], and adjusted heterophily [53], and are all designed for homogeneous graphs. To apply these three measures to our proposed heterogeneous heterophilic graphs, we convert the graphs to homogeneous graphs by removing the type information on nodes and edges. Generally, existing heterophily measures (e.g., edge heterophily, node heterophily, and adjusted heterophily) are defined based only on connections between nodes with labels. For example, in academic networks, only "paper" nodes are labeled. Therefore, only edges connecting "paper→paper" are used to define and calculate heterophily. From the measurements presented in Table 4, we observe that five of the datasets (ogbn-mag, mag-year, oag-cs, oag-eng, oag-chem) exhibit high edge and node heterophily, while RCDD, IEEE-CIS-G, H-Pokec, and PDNS exhibit lower values. Interestingly, the latter four datasets consist of binary class labels and some have high class imbalance. It was shown by Lim et al. [41] that edge and node heterophily are sensitive to the number of classes and class imbalance. We therefore apply the more reliable class-insensitive adjusted heterophily measure [53]. Note that a value of adjusted heterophily close to 0 indicates that nodes predominantly connect to nodes of the same class, exhibiting homophily. A value approaching or exceeding 1 suggests that nodes are more likely to connect to nodes of different classes, demonstrating heterophily. From the adjusted heterophily measure shown in Table 4, we can confirm that RCDD, IEEE-CIS-G, H-Pokec, and PDNS datasets are actually heterophilic.

However, it is important to highlight that these typical heterophily measures are problematic and do not show the whole picture when directly applied to heterogeneous graphs. Standard heterophily measures typically only account for connections between labeled nodes. In our heterogeneous graphs, only a single type of node (*task entity*) is tagged with a label. For instance, in datasets where only "paper" nodes carry labels, these measures evaluate heterophily based on interactions among just "paper" nodes, ignoring a significant portion of the graph structure that includes other node types and connections. Consequently, these approaches overlook the rich and varied inter-node relationships, such as complex metapaths like "paper→author→paper" that involve multiple node types. Heterogeneous homophilic GNNs can exploit hidden homophily within complex metapaths to achieve effective performance, as observed by Guo et al. [21]. However, conventional metrics that misleadingly indicate high heterophily can be deceptive, suggesting that these GNNs are effective at handling heterophilic graphs when, in fact, they are capitalizing on the underlying homophilic relationships. For example, the traditional heterophily score, adjusted heterophily, for the IEEE-CIS-G dataset is 1.3151 as shown in Table 4 indicating a challenge for GNNs designed for homophilic graphs. However, when we apply our newly proposed \mathcal{H}^2 index, which accounts for diverse metapaths, the adjusted score is 0.9846 as shown in Table 1, revealing less overall heterophily. This disparity highlights the limitations of existing heterophily measures when applied to heterogeneous graph contexts and shows the necessity for more nuanced evaluation metrics.

E Experiment Setup

We implement our methods and run experiments using PyTorch 2.0.1 [50] (3-clause BSD license) in Python 3.9, and make heavy use of the PyTorch Geometric library 2.5.0 [14] (MIT license) for graph representation learning. We built UNIFIEDGT upon the popular GraphGym library [75] (MIT license), which has comprehensive machine learning components, flexible experiment configurations, and an extendable component registry. We also provide experiment configuration files that can be used to reproduce the experiment results reported in this paper. All of the model training and data processing were performed on machines with an Nvidia V100 GPU with 32GB of memory, provided by the Satori IBM Power9 cluster at the Massachusetts Institute of Technology.

E.1 Further Details of Baselines

In this section, we provide more detailed information on the baseline models. We categorize these methods into five main groups: (1) *Methods using only node features*. (2) *Methods using only graph structure*. (3) *Homogeneous homophilic GNNs*. (4) *Homogeneous heterophilic GNNs*. (5) *Heterogeneous homophilic GNNs*.

- (1) **Methods using only node features.** These models rely solely on the attributes of the nodes without considering graph topology.
 - **MLP** [18]: A basic neural network model that processes node features without considering the graph structure.
- (2) **Methods using only graph structure.** Methods in this category includes models using the graph structural connections to diffuse information, but does not explicitly use node or edge features. These models perform graph-based operations that focus on the connectivity pattern among nodes to propagate labels or features.
 - **Label propagation** [82, 51]: A semi-supervised technique that spreads labels through the graph based on its structure.
 - **SGC** [68]: A simplified graph convolution network by removing non-linearities and reducing the complexity of model training on graph-structured data.
- (3) **Homogeneous Homophilic GNNs.** Methods in this category is designed for graphs where all nodes and edges are of a single type. These models are optimized for scenarios where connected nodes typically share similar labels or attributes. They leverage both node features and graph structure.
 - **GCN** [32]: A GNN that uses a localized first-order approximation of spectral graph convolutions, effectively leveraging the graph structure and node features.
 - **GraphSAGE** [22]: A GNN that employs a sampling and aggregation framework to efficiently generate node embeddings. It concatenates the self-node features with neighbors' features and has been shown to perform well when the graph has some heterophily [83].
 - **GAT** [64]: A GNN that employs the attention mechanism to weight the significance of neighbors.
 - **GIN** [70]: A GNN designed to capture the power of the Weisfeiler-Lehman graph isomorphism test by using a sum aggregator to update the node representations.
 - **APPNP** [16]: A GNN that combines the propagation of labels throughout a graph with a personalized PageRank scheme for effective learning.
 - **NAGphormer** [9]: A transformer-based GNN that integrates node features and graph topology through attention mechanisms, enhancing model flexibility and scalability.
- (4) **Homogeneous Heterophilic GNNs.** Methods in this category is optimized for graphs where connected nodes are likely to have different labels or attributes. These models specifically challenge the common homophily assumption and are designed for homogeneous graphs.
 - **MixHop** [1]: A heterophilic GNN that aggregates features from a node's neighbors at various distances, allowing the model to learn more complex patterns of heterophily.
 - **FAGCN** [7]: A heterophilic GNN that focuses on adapting the aggregation mechanisms to better handle the heterophily inherent in some graphs by modulating the influence of neighboring nodes based on their label discrepancy.
 - **ACM-GCN** [44]: A heterophilic GNN designed to address heterophily by enhancing the model's ability to discriminate between different types of node relationships.
 - **LINKX** [41]: A heterophilic GNN that decouples structure and feature transformation, making it simple and scalable.
 - **LSGNN** [10]: A heterophilic GNN that models heterophily using local similarity and has been shown to outperform other powerful heterophilic GNN, like GloGNN [40].
- (5) **Heterogeneous Homophilic GNNs.** Methods in this category is optimized for graphs with multiple types of nodes and edges, but still assume homophily among connections. They manage the complexity of the varied entities and relation types within the graph.
 - **RGCN** [57]: A heterogeneous GNN that introduces relation-specific transformations to separately aggregate neighbors based on relations.
 - **RGraphSAGE**: a heterogeneous GNN that extends GraphSAGE to handle heterogeneous graphs by incorporating edge-type information into the aggregation process.

- **RGAT**: A heterogeneous GNN that adapts the GAT framework to heterogeneous graphs, integrating relational attention into its computation.
- **HAN** [66]: A heterogeneous GNN that applies both node-level and semantic-level attention, focusing on information aggregation along different metapaths.
- **HGT** [29]: A heterogeneous GNN that introduces a type-aware attention mechanism to learn node and edge type-dependent representations.
- **SHGN** [45]: A heterogeneous GNN that enhances node representation learning by leveraging type-specific embeddings, incorporating attention mechanisms and residual connections, and applying an ℓ_2 -norm to the output for regularization and stability.
- **HINormer** [46]: A heterogeneous GNN that capitalizes on a large-range aggregation mechanism for node representation learning by using a local structure encoder and a heterogeneous relation encoder.

E.2 Implementation Details.

In this section, we elaborate on the details of the framework and experiment implementation.

1. **Experiment Configurations.** For reproducibility, the specific experimental settings that yielded the best results for each dataset are documented in Table 5. They are also available as configuration files provided in the open-source library at <https://github.com/junhongmit/H2GB/>. The hyperparameters of each model were initially set based on the authors’ official experimental settings and subsequently fine-tuned in our experiments for optimal performance. To ensure fairness, we fixed the graph sampling parameters for all baseline models on each dataset, ensuring that each model was exposed to the same amount of graph data during training.
2. **Minibatching and Memory Management**
 - **Minibatching.** Many of the existing heterophilic GNNs are generally designed and trained on relatively small graphs, and do not scale well to large graphs. To avoid out-of-memory errors, we implement minibatching strategies to train the baseline models. This approach is critical for handling models traditionally designed for smaller graphs. Instead of feeding the entire graph into the model, the minibatching approach samples a local subgraph around the target nodes. We keep the sampling parameters the same for each dataset to ensure each model has a similar view of the dataset to ensure fair comparison.
3. **Graph Encoding and Feature Handling**
 - **Automatic Node Feature Embedding.** For nodes with no input features, such as in H-Pokec and IEEE-CIS, our graph encoding component automatically adds a learnable embedding to each node type. This step is critical for all of the GT methods, which rely highly on attention calculated between connected node features.
 - **Feature Projection.** An embedding layer is applied to linearly project node features onto a unified embedding space.
4. **Graph Structure and Message Passing**
 - **Homogeneous GNNs Adaptation to Heterogeneous Context.** While the PyTorch Geometric Library provides an implementation of Relational-GCN, it does not extend this support to other GNN models for heterogeneous graphs. To bridge this gap, we utilize generic heterogeneous GNN wrappers available within the library to adapt two widely-used homogeneous GNN models, GraphSAGE and GAT, for heterogeneous graph settings. This results in Relational-GraphSAGE (R-GraphSAGE) and Relational-GAT (R-GAT), respectively. These wrappers instantiate distinct GNN layers for each edge type, allowing for dedicated message passing for each relation. This approach ensures that information is processed differently across various edge types, extending the model to handle the complexities of heterogeneous data.
 - **Handling Heterogeneous Structures in Cross-Type Heterogeneous Attention.** Note that popular graph learning libraries, like PyTorch Geometric Library and Deep Graph Library (DGL), often store the edges of each metarelation in separate adjacency lists to facilitate metarelation-based message passing. This data storage format significantly decreases the running time efficiency of cross-type communication and requires more computations. We provide an optimized implementation of the cross-type heterogeneous attention in our open-source library to support the cross-type communication in our attention mechanism. This implementation leverages the inherent sparsity of the masked attention mechanism, using sparse tensor operations to enhance computational efficiency.

5. *Attention Mechanisms*

- **SHGN Model Configuration.** For the SHGN model, we noticed that the usage of the attention residuals mechanism and application of ℓ_2 -normalization are not always effective. When incorporating them into the model, the model is unable to learn meaningful representations on the RCDD dataset. We, therefore, omit them for RCDD dataset. We also observe that the 4-layer SHGN does not converge in the oag-cs, oag-eng, and oag-chem datasets, which may be due to the lack of normalization layers. We therefore use a 3-layer SHGN model for these datasets.

6. *Optimization and Learning Rate Scheduling*

- **Optimizer and Scheduler.** All experiments use the AdamW optimizer paired with a cosine annealing learning rate scheduler with warmup [43] to optimize training convergence. Learning rates are listed in Table 5 and weight decays are all set to 10^{-5} .
- **Class Weight Adjustment.** For the IEEE-CIS-G dataset, we apply a weighted cross-entropy loss with the minority class weights set to 5, while the majority class weight is set to 1 to alleviate class imbalance issues. The specific value is selected based on the overall baseline performance.

Table 5: Summary of the hyperparameters of every model on our datasets. The sample sizes are represented using the format of $n \times d$, where n is the number of sampled neighbors per iteration, and d is the number of sampling iterations.

		ogbn-mag	mag-year	oag-cs	oag-eng	oag-chem	H-Pokec	RCDD	IEEE-CIS-G	PDNS
Sampling Parameters	Sampling Method Sample Sizes	512 × 6	512 × 6	64 × 6	64 × 6	64 × 6	128 × 3	256 × 4	64 × 6	256 × 4
MLP	d_{hid}	512	512	256	256	256	256	256	128	64
	# Layers	3	3	3	3	3	3	3	2	2
	Normalization	Batch	Batch	Batch	Batch	Batch	Batch	Batch	Batch	Batch
	Dropout	.2	.2	.2	.2	.2	.0	.0	.5	.2
LP	α Iterations					0.1 50				
SGC	α					0.1				
GCN/ GraphSAGE/ GAT/ GIN/ MixHop/ FAGCN	d_{hid} # Layers # Heads Normalization Dropout Learning rate	512 4 8 Batch .2 .001	512 4 8 Batch .2 .001	256 3 4 Batch .2 .005	256 3 4 Batch .2 .001	256 3 8 Batch .2 .005	256 3 8 Batch .5 .001	256 3 8 Batch .2 .001	128 3 8 Batch .5 .001	64 3 8 Batch .2 .001
APPNP	α K d_{hid}	3 512	4 512	2 256	3 256	3 256	3 256	3 256	3 128	4 64
	Normalization	Batch	Batch	Batch	Batch	Batch	Batch	Batch	Batch	Batch
	Dropout	.2	.2	.2	.2	.5	.2	.2	.5	.2
	Learning rate	.001	.001	.005	.001	.005	.001	.001	.001	.001
NAGphormer	d_{hid} Hops # Layers # Heads	512 7 4 8	512 7 4 8	256 6 3 8	256 6 3 8	256 6 3 8	256 7 3 8	256 5 3 8	128 3 3 8	64 6 3 8
	Normalization	Batch	Batch	Batch	Batch	Batch	Batch	Batch	Batch	Batch
	Dropout	.2	.2	.2	.2	.2	.5	.2	.5	.2
	Learning rate	.001	.001	.005	.001	.005	.001	.001	.001	.001
GraphTrans	d_{GNN} # GNN layers d_{hid} # GT layers # Heads	128 3 512 4 8	128 3 512 4 8	128 3 256 3 8	128 3 256 3 8	128 3 256 3 8	128 3 256 3 8	128 3 256 3 8	64 3 128 3 8	32 3 64 3 8
	Normalization	Layer	Layer	Layer	Layer	Layer	Layer	Layer	Layer	Layer
	Dropout	.2	.2	.2	.2	.2	.5	.2	.5	.2
	Learning rate	.0005	.0005	.0005	.0005	.0005	.0005	.0005	.0005	.0005
Gophormer	d_{hid} Hops # GT layers # Heads # Global nodes	256 2 3 8 2	256 2 3 8 2	256 2 3 8 2	256 2 3 8 2	256 2 3 8 2	128 2 3 8 2	256 2 3 8 2	128 2 3 8 2	64 2 3 8 2
	Normalization	Layer	Layer	Layer	Layer	Layer	Layer	Layer	Layer	Layer
	Dropout	.2	.2	.2	.2	.2	.5	.2	.5	.2
	Learning rate	.0005	.0005	.0005	.0005	.0005	.0005	.0005	.0005	.0005
LINKX	d_{hid} # MLP layers Dropout Learning rate	512 1 .2 .001	512 1 .2 .001	256 1 .2 .001	256 1 .2 .001	256 1 .2 .001	256 1 .5 .001	256 1 .2 .001	128 1 .5 .001	64 1 .2 .001
ACM-GCN	d_{hid} # Layers Dropout Learning rate	512 4 .5 .001	512 4 .5 .001	256 3 .5 .001	256 3 .5 .001	256 3 .5 .001	256 3 .5 .001	256 3 .5 .001	128 3 .5 .001	64 3 .5 .001
LSGNN	d_{hid} # Reduce layers Dropout Learning rate	512 2 .5 .001	512 2 .5 .001	256 2 .5 .001	256 2 .5 .001	256 2 .5 .001	256 3 .5 .001	256 3 .2 .001	128 3 .5 .001	64 3 .5 .001
GOAT	d_{hid} # Layers # Heads Normalization Dropout Learning rate	128 3 8 Batch .2 .0005	128 3 8 Batch .2 .0005	128 3 8 Batch .2 .0005	128 3 8 Batch .2 .0005	128 3 8 Batch .2 .0005	128 3 8 Batch .5 .0005	128 3 8 Batch .2 .0005	64 3 8 Batch .5 .0005	64 3 8 Batch .2 .0005
R-GCN/ R-GraphSAGE/ R-GAT	d_{hid} # Layers # Heads Normalization Dropout Learning rate	512 4 8 Batch .2 .001	512 4 8 Batch .2 .001	256 3 4 Batch .2 .005	256 3 4 Batch .2 .001	256 3 8 Batch .2 .005	256 3 8 Batch .5 .001	256 3 8 Batch .2 .001	128 3 8 Batch .5 .001	64 3 8 Batch .2 .001
HAN/ HGT/ SHGN	d_{hid} # Layers # Heads Normalization Dropout Learning rate	512 4 8 Batch .2 .0005	512 4 8 Batch .2 .0005	256 3 8 Batch .2 .001	256 3 8 Batch .2 .001	256 3 8 Batch .2 .001	256 3 8 Batch .5 .0005	256 3 8 Batch .2 .0005	128 3 8 Batch .5 .001	64 3 8 Batch .2 .0005
\mathcal{H}^2 G-former	d_{hid} # Layers # Heads Normalization Dropout Learning rate	512 3 8 Layer .2 .0005	512 3 8 Layer .5 .0005	256 3 8 Layer .2 .0005	256 3 8 Layer .2 .0005	256 3 8 Layer .2 .0005	256 3 8 Layer .5 .0005	256 3 8 Layer .2 .0005	128 3 8 Layer .5 .001	64 3 8 Layer .0 .0005